

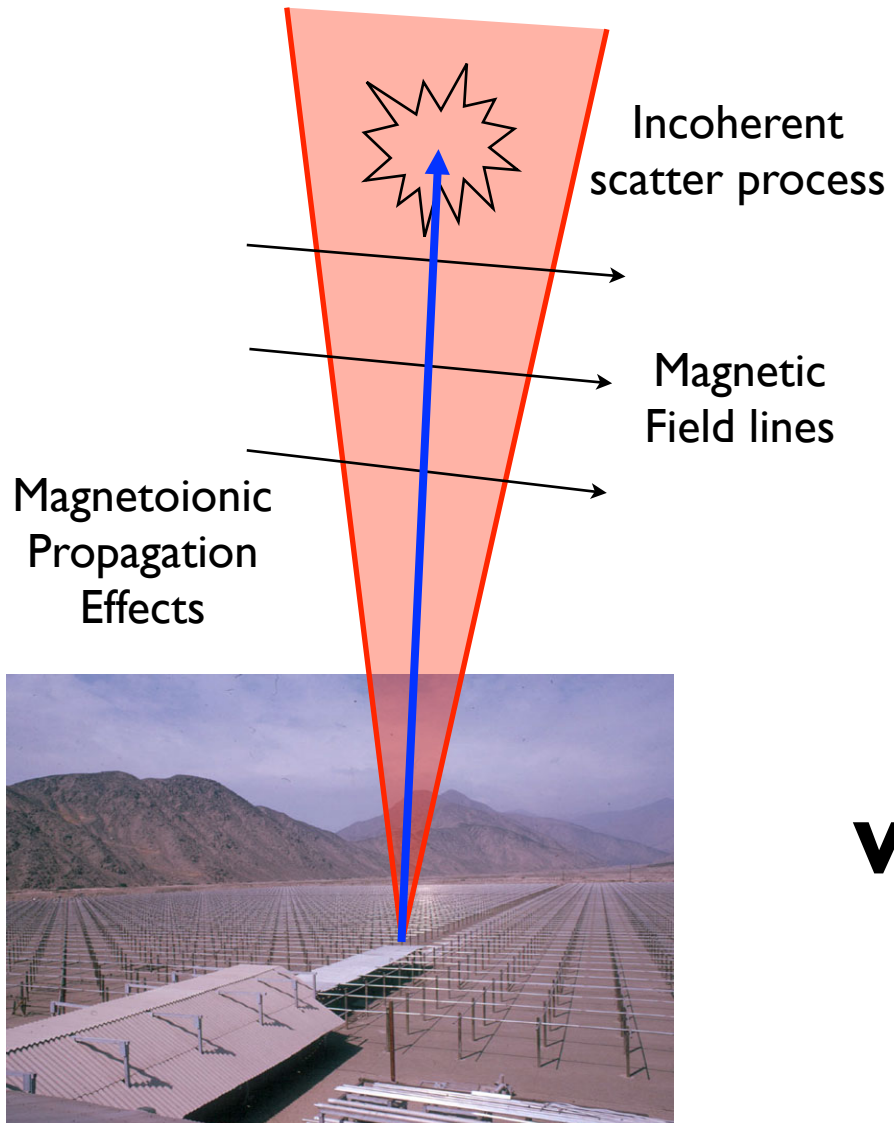


Study of Coulomb collisions and magneto-ionic propagation effects on ISR measurements at Jicamarca

Marco A. Milla
Jicamarca Radio Observatory
JIREP Program



Jicamarca ISR measurements perp. to B



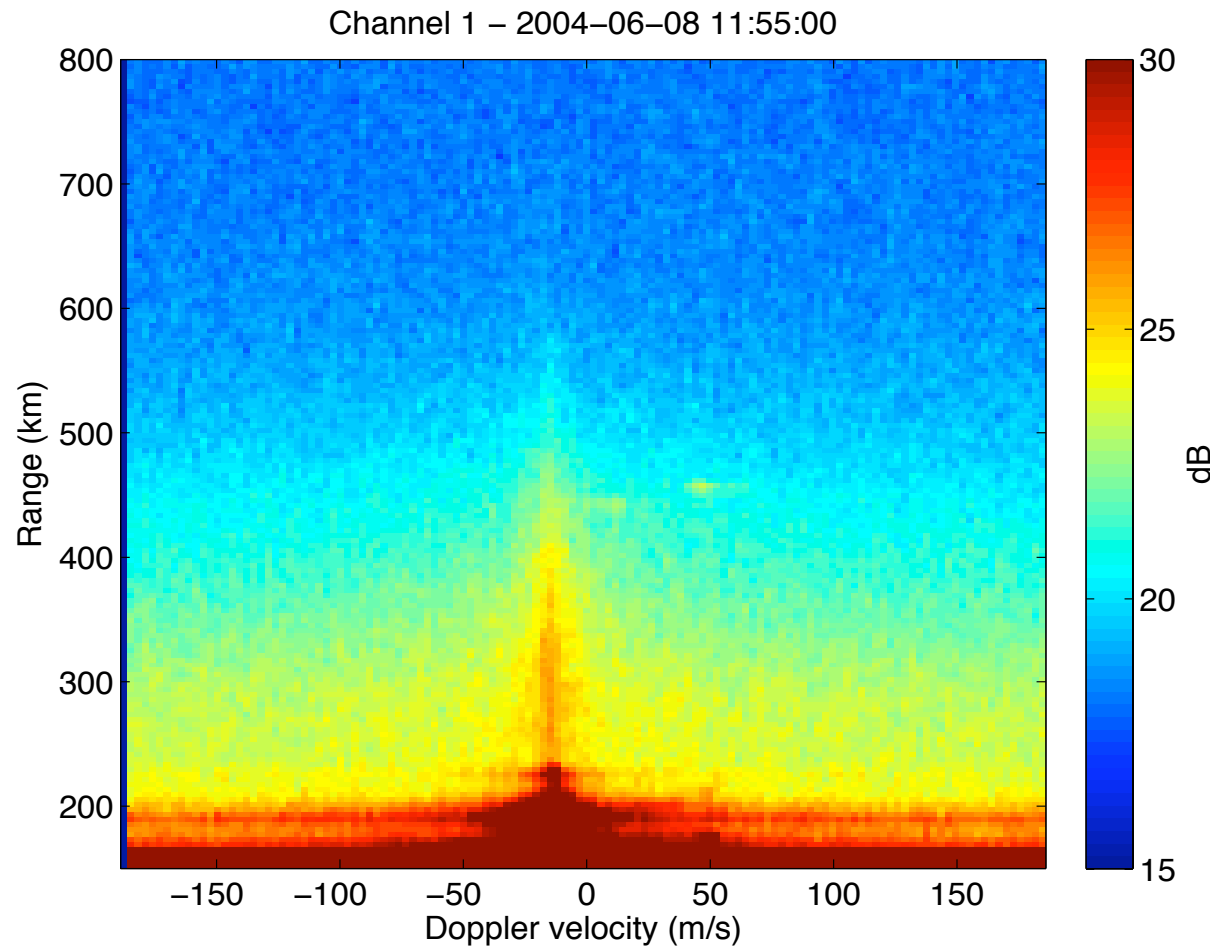
Physical parameters that can be measured:

- Drifts: using Kudeki et al (1999) spectral fitting technique (Doppler shift of ISR spectrum).
- Densities: using the “Differential-phase” technique developed by Kudeki et al (2003).

What about temperatures?

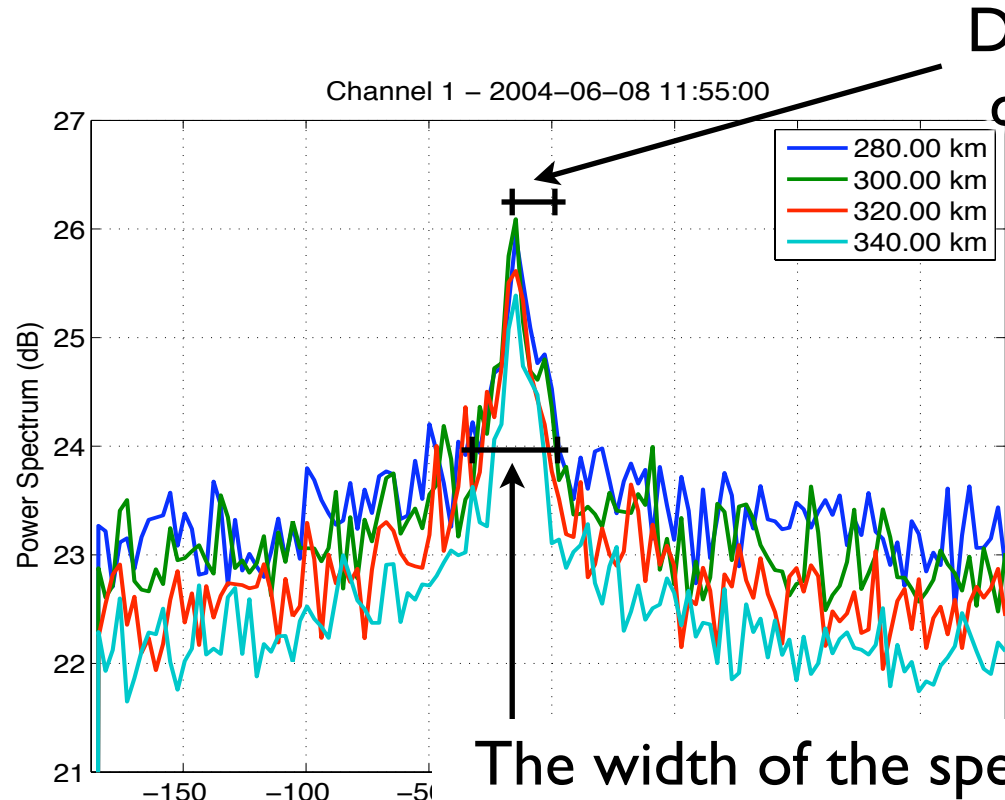


Jicamarca ISR spectrum perp. to B





Jicamarca ISR spectrum perp. to B

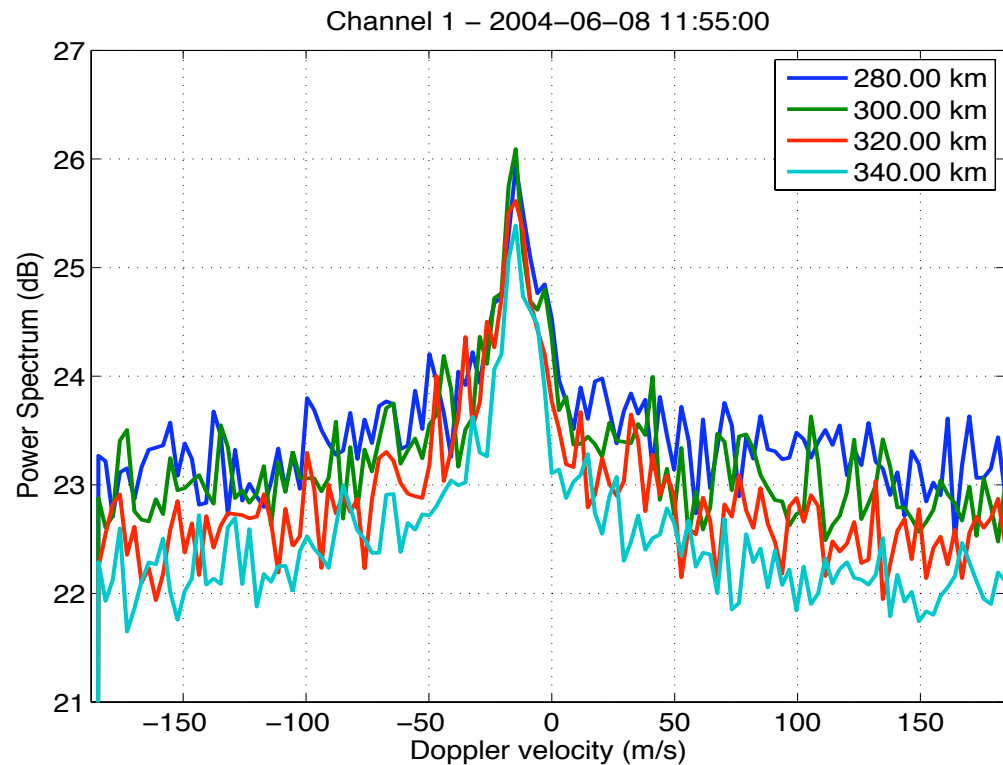


Doppler shift of the spectrum is a direct measurement of the drift.

The width of the spectrum contains information about the temperatures.



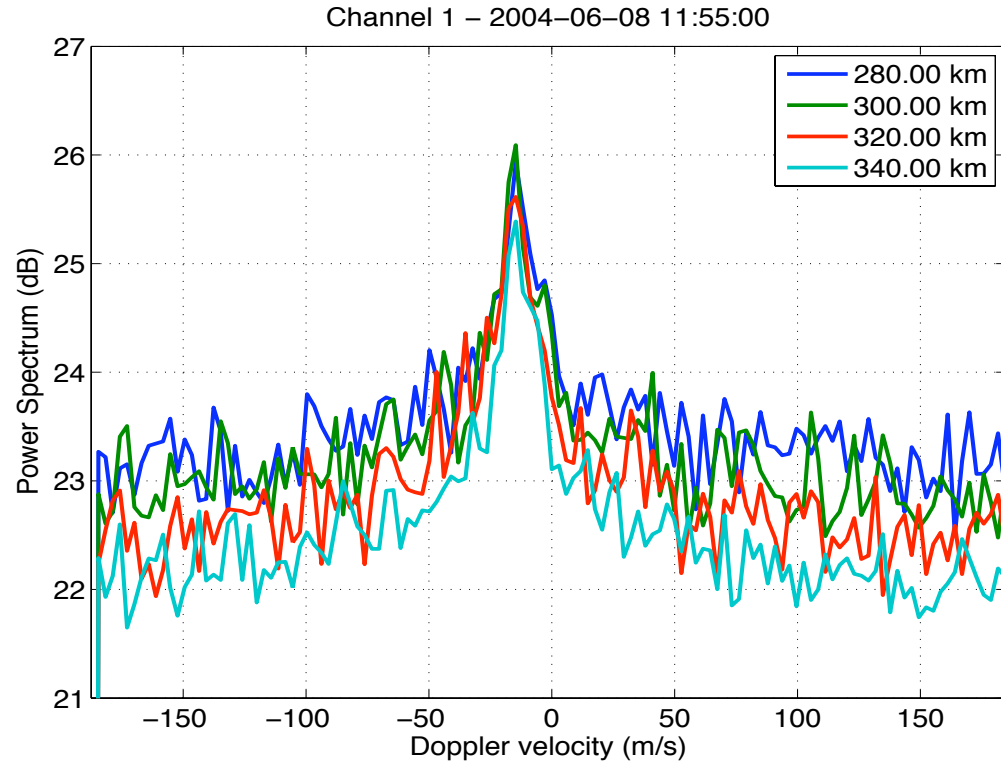
Jicamarca ISR spectrum perp. to B



Kudeki et al (1999) fitted the measurements using a simplified spectral model. This model was developed based on the collisionless IS theory. But, the temperatures they obtained were about half of what is expected.



Jicamarca ISR spectrum perp. to B



Kudeki et al (1999) fitted the measurements using a simplified spectral model. This model was developed based on the collisionless IS theory. But, the temperatures they obtained were about half of what is expected.

The measured spectrum was narrower than what the collisionless theory predicts, and therefore, a revision of the IS theory for modes propagating perpendicular to B was needed.



Research project

- Main goal: To develop an incoherent scatter spectrum model for modes propagating perpendicular to B .
- This project is divided in two stages.
 - Study of the effects of Coulomb collisions
 - Modeling the magnetoionic propagation effects
- Future Application: The estimation of ionospheric temperatures with Jicamarca antenna beams pointed perpendicular to B .



First stage:

Modeling the incoherent scatter
spectrum considering the effects of
Coulomb collisions



IS spectrum and Gordeyev integrals

- Spectrum of electron density fluctuations (e.g., Kudeki & Milla, 2010)

$$\langle |n_e(\vec{k}, \omega)|^2 \rangle = \frac{|j\omega\epsilon_o + \sigma_i(\vec{k}, \omega)|^2 \langle |n_{te}(\vec{k}, \omega)|^2 \rangle + |\sigma_e(\vec{k}, \omega)|^2 \langle |n_{ti}(\vec{k}, \omega)|^2 \rangle}{|j\omega\epsilon_o + \sigma_e(\vec{k}, \omega) + \sigma_i(\vec{k}, \omega)|^2}$$

- In terms of the Gordeyev integrals, the spectra of thermal density fluctuations and the conductivities are given by

$$\frac{\langle |n_{ts}(\vec{k}, \omega)|^2 \rangle}{N_s} = 2\text{Re}\{J_s(\omega)\} \quad \frac{\sigma_s(\omega, \vec{k})}{j\omega\epsilon_o} = \frac{1 - j\omega J_s(\omega)}{k^2 h_s^2}$$

- The Gordeyev integral is the one-sided Fourier transform of the single particle ACF (Hagfors & Brockelman, 1971)

$$J_s(\omega) = \int_0^\infty d\tau e^{-j\omega\tau} \langle e^{j\vec{k} \cdot \Delta \vec{r}_s} \rangle \quad \langle e^{j\vec{k} \cdot \Delta \vec{r}_s} \rangle = \langle e^{j\vec{k} \cdot (\vec{r}_s(t+\tau) - \vec{r}_s(t))} \rangle$$



Langevin equation and particle trajectories

- Instead of solving the Boltzmann kinetic equation with the Fokker-Planck collision operator to determine the pdf of the particle displacements, we model the particle motion by a set of Generalized Langevin equations:

$$\begin{aligned}\frac{d\vec{v}(t)}{dt} &= \frac{q}{m} \vec{v}(t) \times \vec{B} - \beta(v) \vec{v}(t) + \sqrt{D_{\parallel}(v)} \mathcal{W}_1(t) \hat{v}_{\parallel}(t) \\ &\quad + \sqrt{\frac{D_{\perp}(v)}{2}} \mathcal{W}_2(t) \hat{v}_{\perp 1}(t) + \sqrt{\frac{D_{\perp}(v)}{2}} \mathcal{W}_3(t) \hat{v}_{\perp 2}(t) \\ \frac{d\vec{r}(t)}{dt} &= \vec{v}(t)\end{aligned}$$

- Coulomb collisions are simulated by a deterministic friction force and random diffusion forces.
- These equations represent an alternative description of the Fokker-Planck collision process (Chandrasekhar, 1943; Gillespie, 1996).
- This approach give us more insight into the physics of the problem.



Computer simulations

- The trajectory of a test particle is simulated using

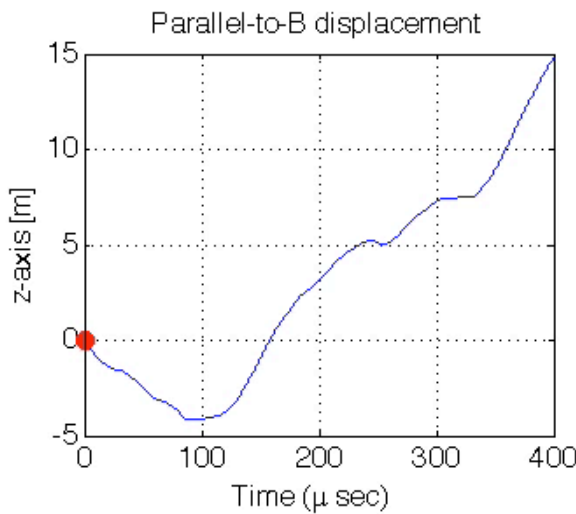
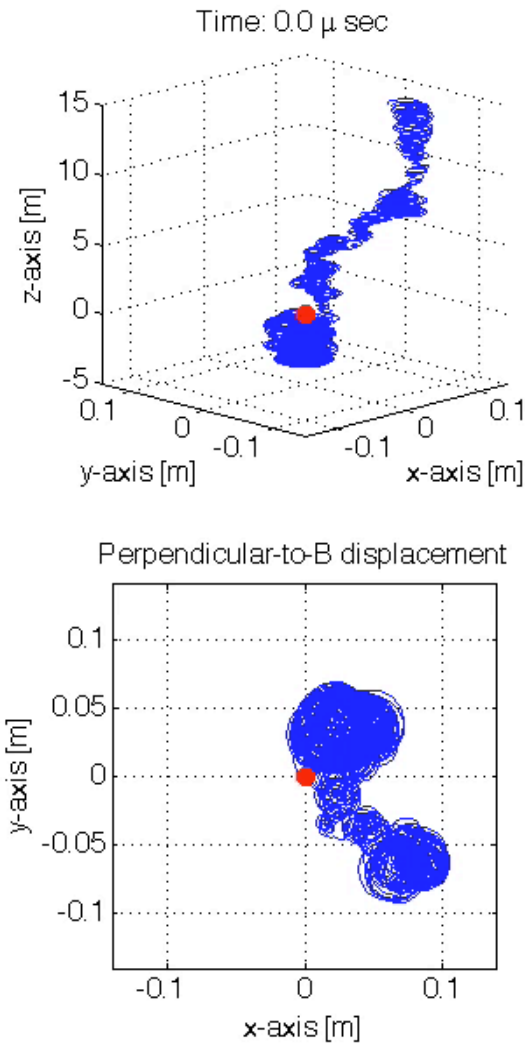
$$\vec{v}_{n+1} = \vec{v}_n + \frac{q}{m} \vec{v}_n \times \vec{B} \Delta t - \beta(v_n) \Delta t \vec{v}_n + \sqrt{D_{\parallel}(v_n) \Delta t} \mathcal{N}_1 \hat{v}_{\parallel} + \sqrt{D_{\perp}(v_n) \frac{\Delta t}{2}} \mathcal{N}_2 \hat{v}_{\perp 1} + \sqrt{D_{\perp}(v_n) \frac{\Delta t}{2}} \mathcal{N}_3 \hat{v}_{\perp 2}$$

$$\vec{r}_{n+1} = \vec{r}_n + \frac{\vec{v}_{n+1} + \vec{v}_n}{2} \Delta t$$

- The Spitzer velocity-dependent friction and diffusion coefficients are used to model the effects of Coulomb collisions.
- Assumption: the magnetic field is weak enough such that within a Debye cube the trajectories of electrons and ions exhibit small curvatures due to the magnetic field.
- For a given plasma configuration, the simulations run for several hours in order to obtain good statistics of the particle trajectories.

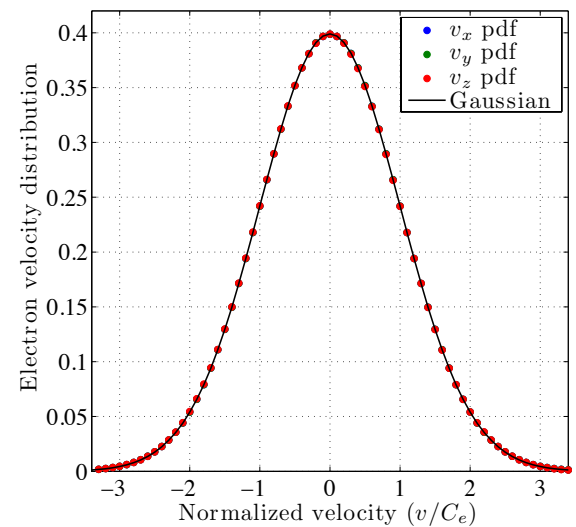


3-D particle trajectories



O+ Plasma:
 $N_e = 10^{12} \text{ m}^{-3}$
 $T_e = 1000 \text{ K}$
 $T_i = 1000 \text{ K}$
 $B = 25\,000 \text{ nT}$

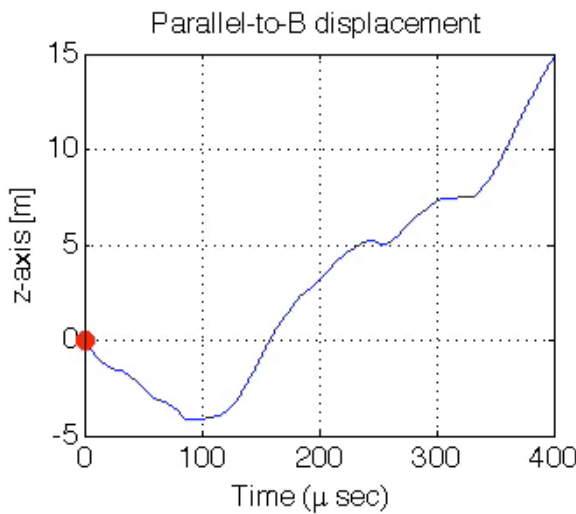
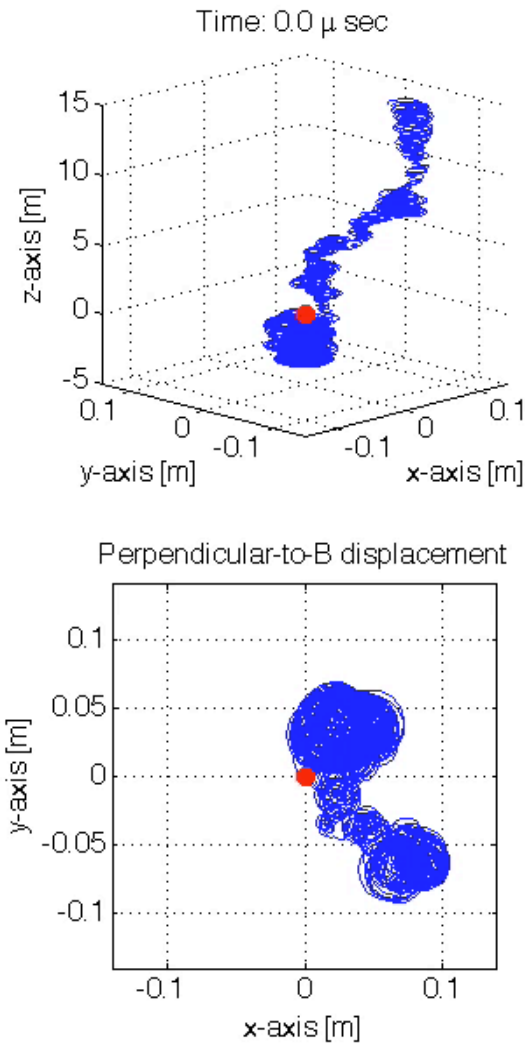
10^4 sequences of 2^{17} samples are generated (30 GB), however, only the statistics (ACF's) are stored (60 MB).



Velocity distributions have a gaussian shape.

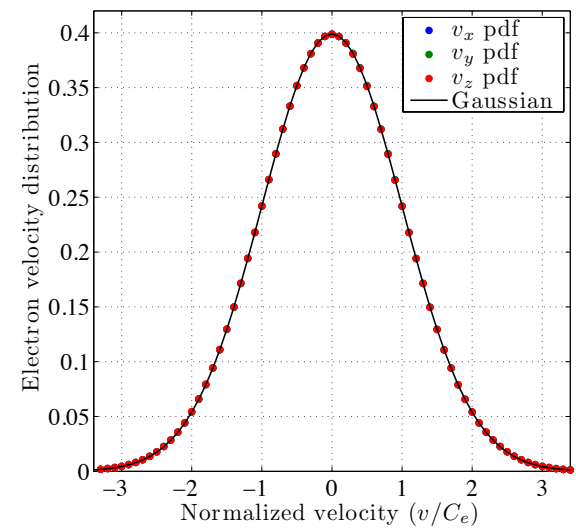


3-D particle trajectories



O+ Plasma:
 $N_e = 10^{12} \text{ m}^{-3}$
 $T_e = 1000 \text{ K}$
 $T_i = 1000 \text{ K}$
 $B = 25\,000 \text{ nT}$

10^4 sequences of 2^{17} samples are generated (30 GB), however, only the statistics (ACF's) are stored (60 MB).



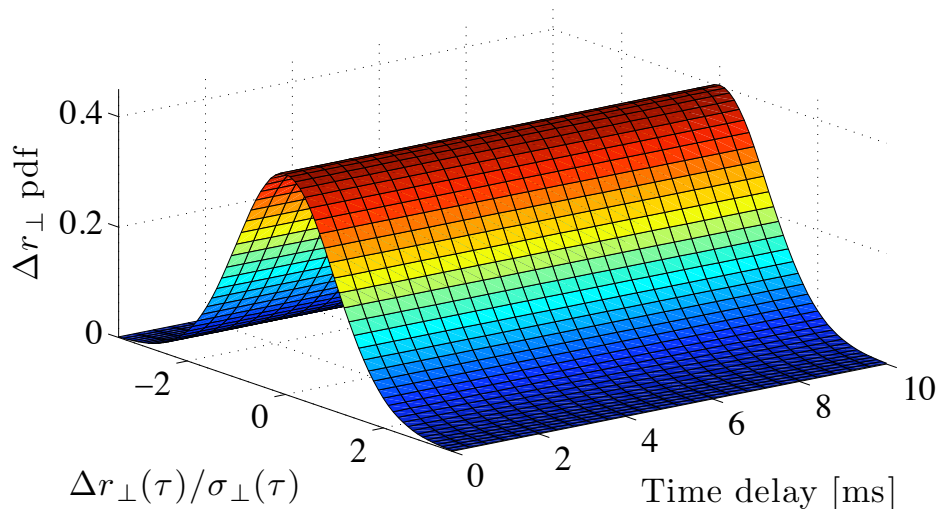
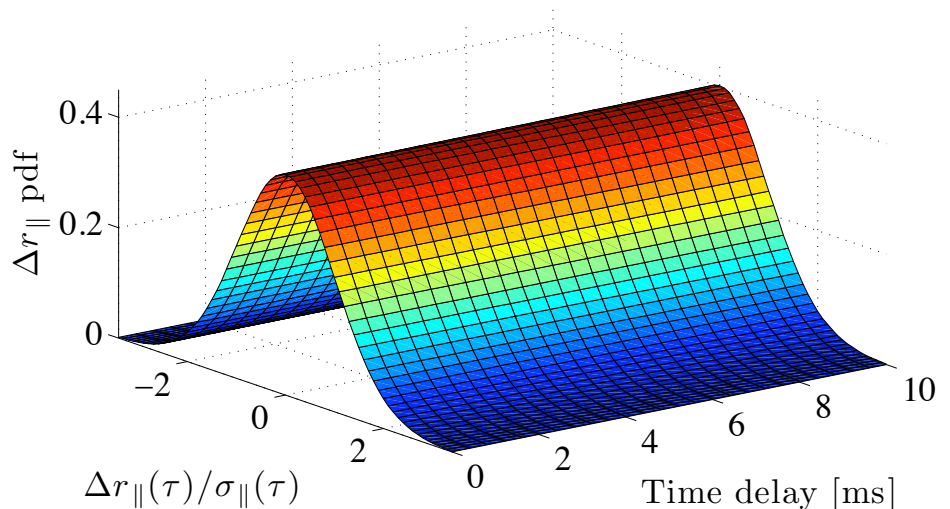
Velocity distributions have a gaussian shape.



Statistics of ion trajectories

- The pdf of the displacement in the direction perpendicular to \mathbf{B} is gaussian as a function of delay τ .
- In the parallel direction, the pdf also looks gaussian.
- A Brownian motion model with Gaussian trajectories is a good representation of the ion motion process (Woodman, 1967).
- The single-ion ACF can be approximated by

$$\left\langle e^{j\vec{k} \cdot \Delta \vec{r}} \right\rangle = e^{-\frac{1}{2}k^2 \sin^2 \alpha \langle \Delta r_{\parallel}^2 \rangle} \times e^{-\frac{1}{2}k^2 \cos^2 \alpha \langle \Delta r_{\perp}^2 \rangle}$$

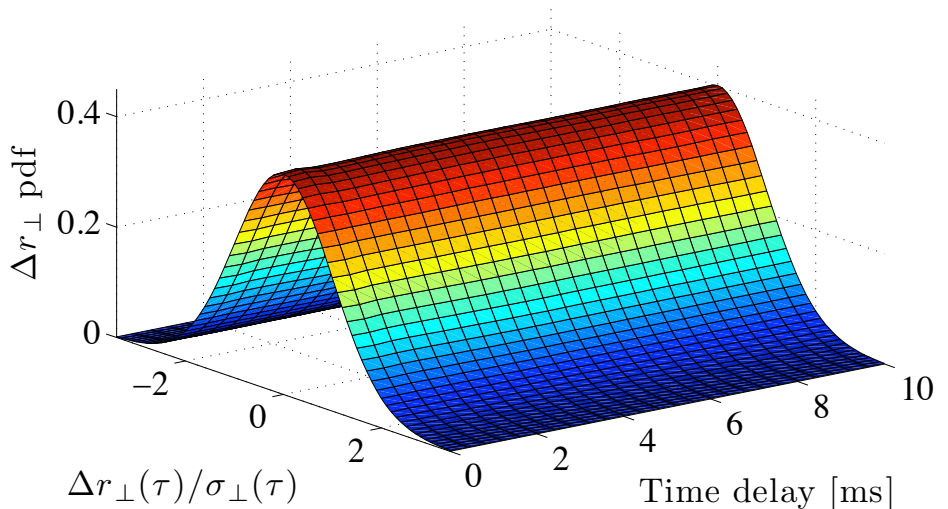
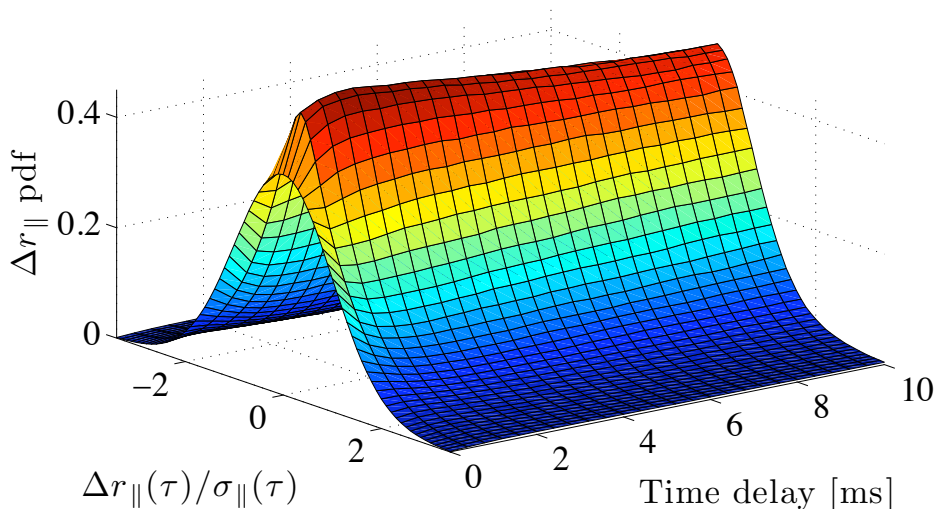
Ion displacement distributions \perp to \mathbf{B} Ion displacement distributions \parallel to \mathbf{B} 



Statistics of electron trajectories

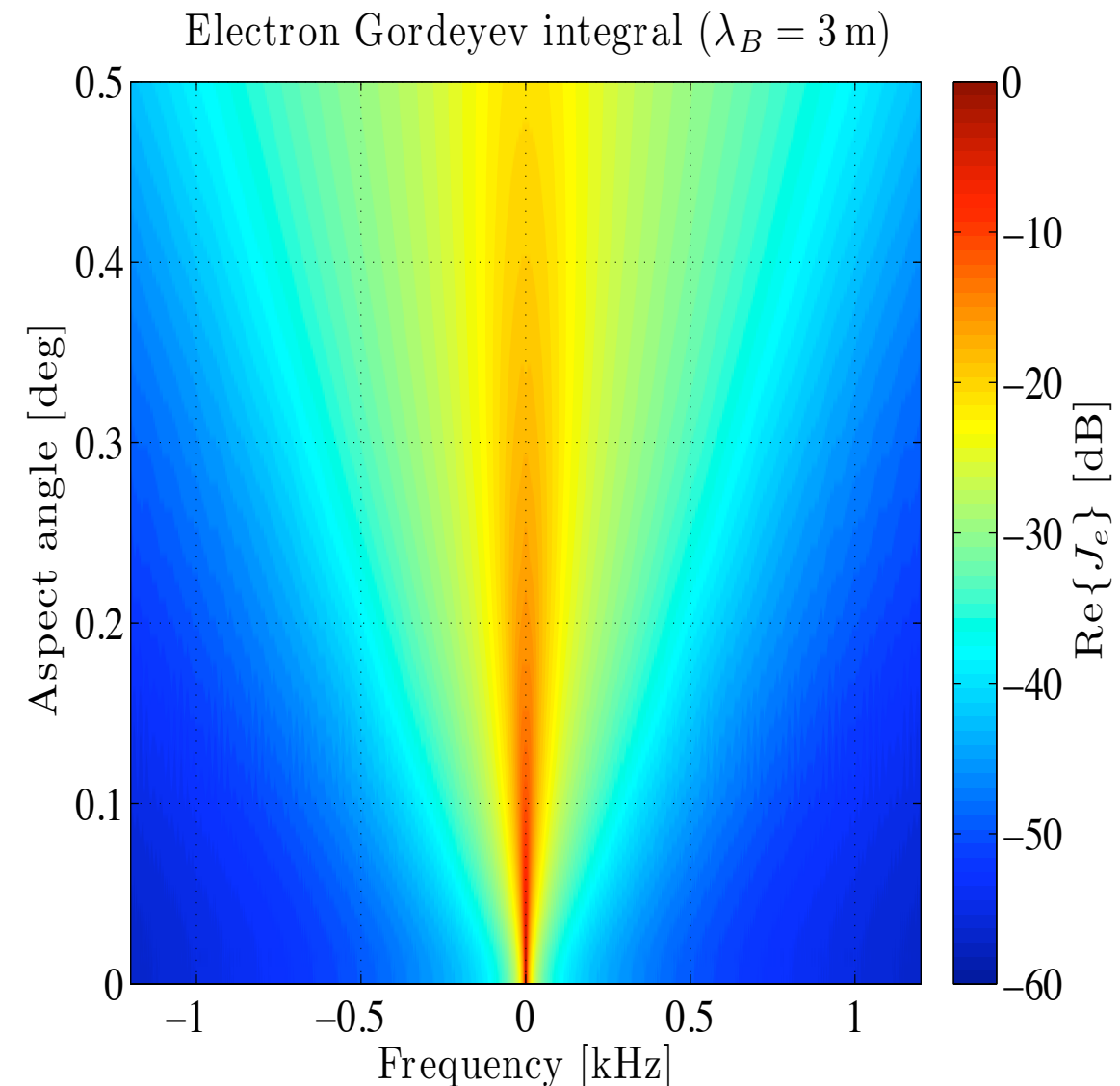
- The pdf of the displacement in the direction perp. to \mathbf{B} is almost gaussian as function of delay τ .
- In the parallel direction, the pdf looks gaussian at short τ , but becomes narrow in less than 1 ms.
- Brownian motion is not a good model for the electrons.
- The components of the electron vector displacement are not independent variables.

$$\left\langle e^{jk \cdot \vec{\Delta r}} \right\rangle = e^{-\frac{1}{2} k^2 \sin^2 \alpha \langle \Delta r_{\parallel}^2 \rangle} \times e^{-\frac{1}{2} k^2 \cos^2 \alpha \langle \Delta r_{\perp}^2 \rangle}$$

Electron displacement distributions \perp to \mathbf{B} Electron displacement distributions \parallel to \mathbf{B} 



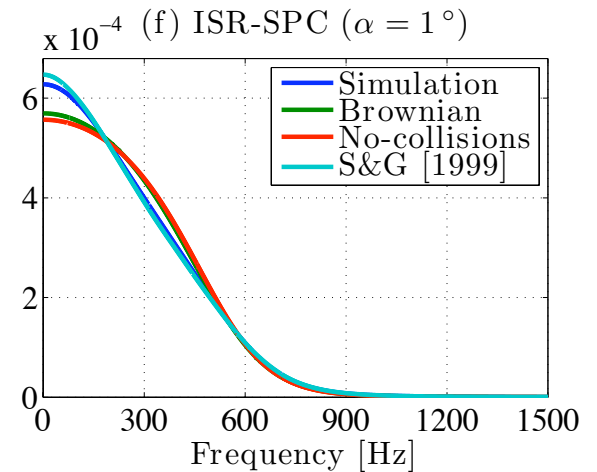
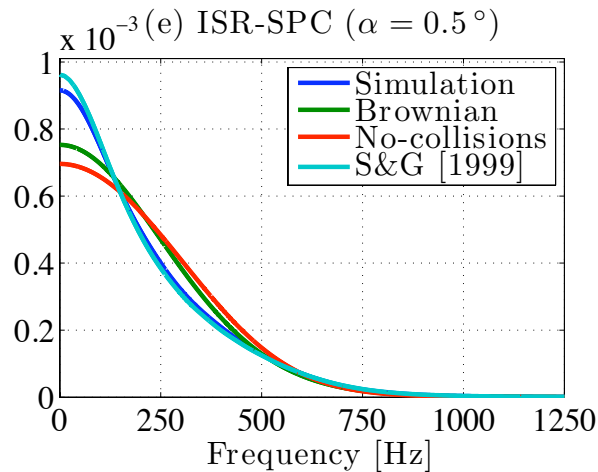
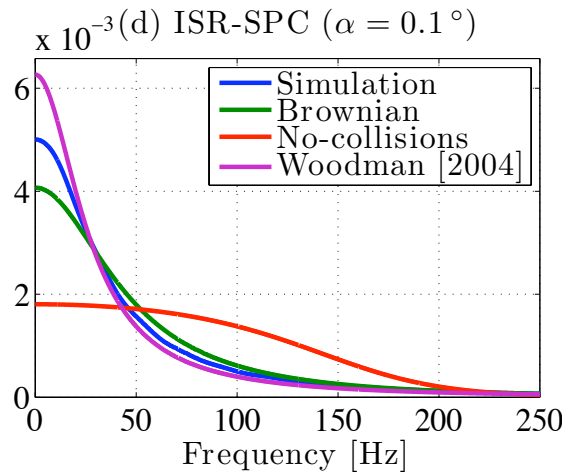
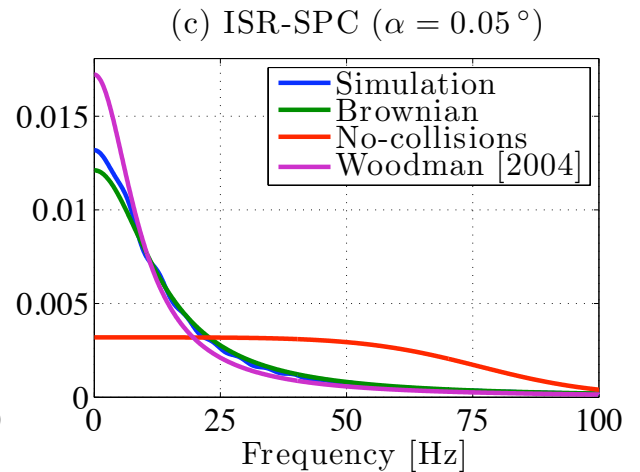
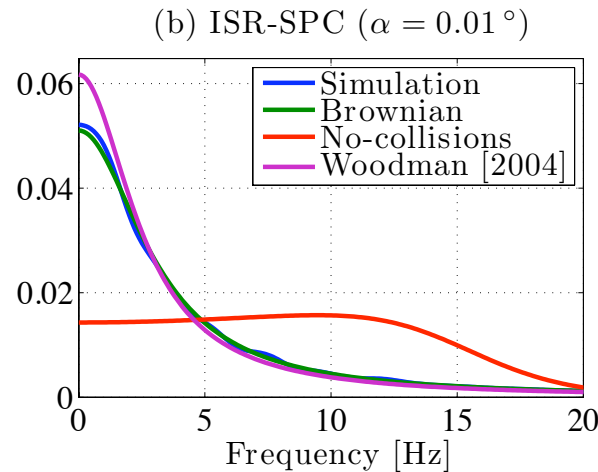
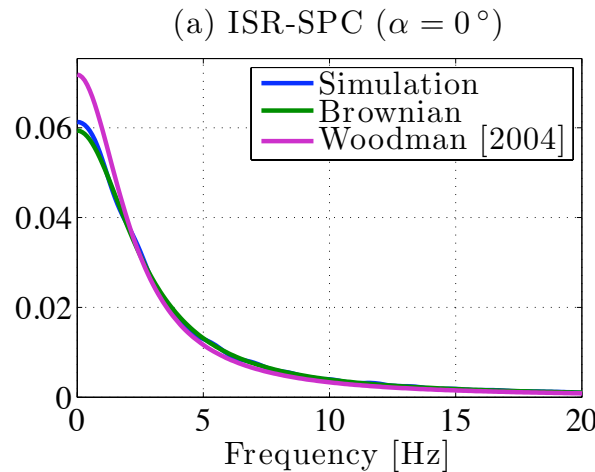
Database of single-electron ACF's



- We have built a library for an oxygen plasma that considers
 - $11 < \log_{10}(Ne) < 13$
 - $600\text{K} < Te < 3000\text{K}$
 - $600\text{K} < Ti < 2000\text{K}$
 - $|B| = 20, 25, 30 \mu\text{T}$
 - Large set of aspect angles from 0° to 90° .
- Electron Gordeyev integrals are computed using the Chirp-Z transform (Li et al, 1991)
- A web-page with the results
[http://collisions.csl.uiuc.edu/
database/gordeyev/](http://collisions.csl.uiuc.edu/database/gordeyev/)



IS collisional spectra (I)

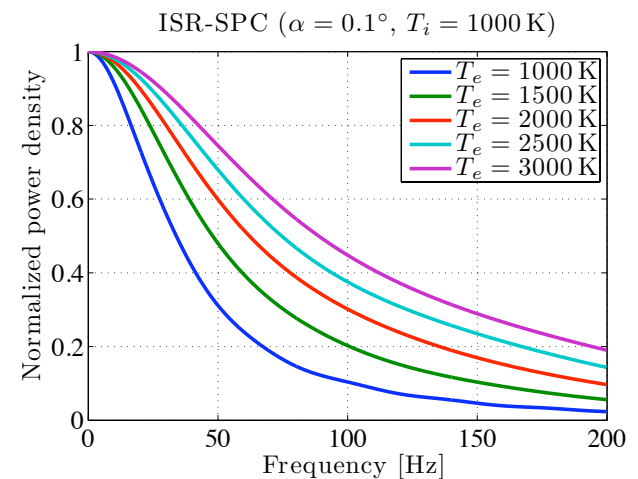
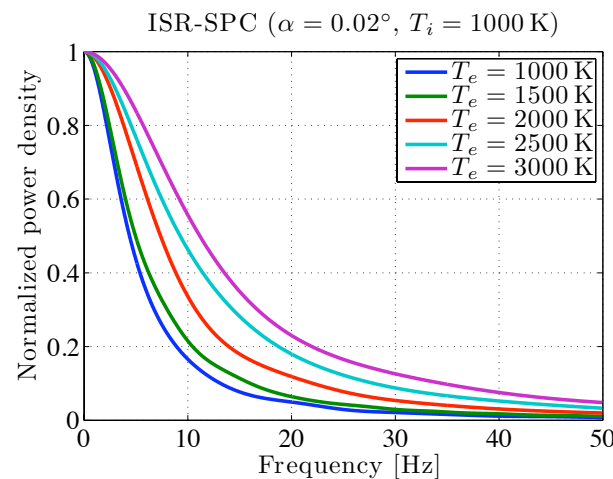
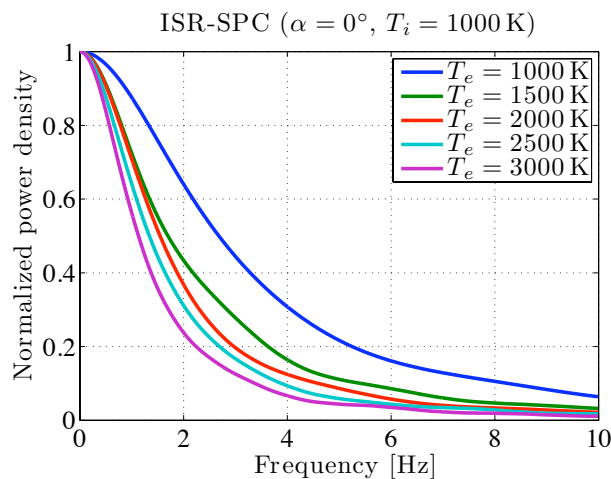
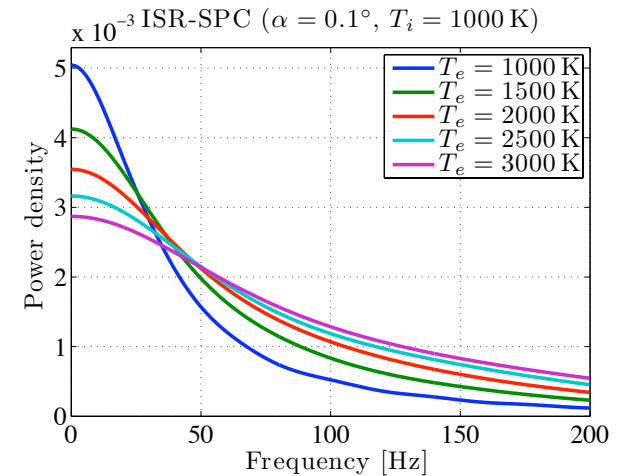
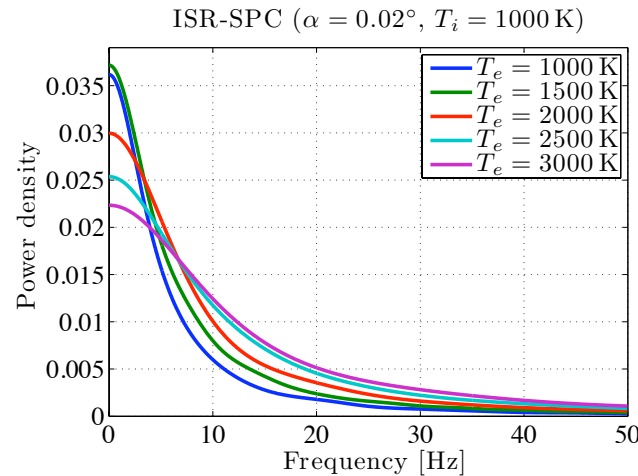
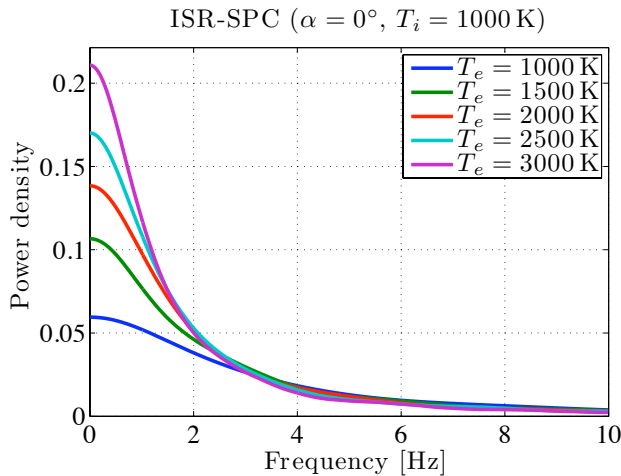


Simulated spectrum at different magnetic aspect angles:

(a) $\alpha=0^\circ$, (b) $\alpha=0.01^\circ$, (c) $\alpha=0.05^\circ$, (d) $\alpha=0.1^\circ$, (e) $\alpha=0.5^\circ$,
and (f) $\alpha=1^\circ$ (Milla & Kudeki, 2010).



IS collisional spectra (2)

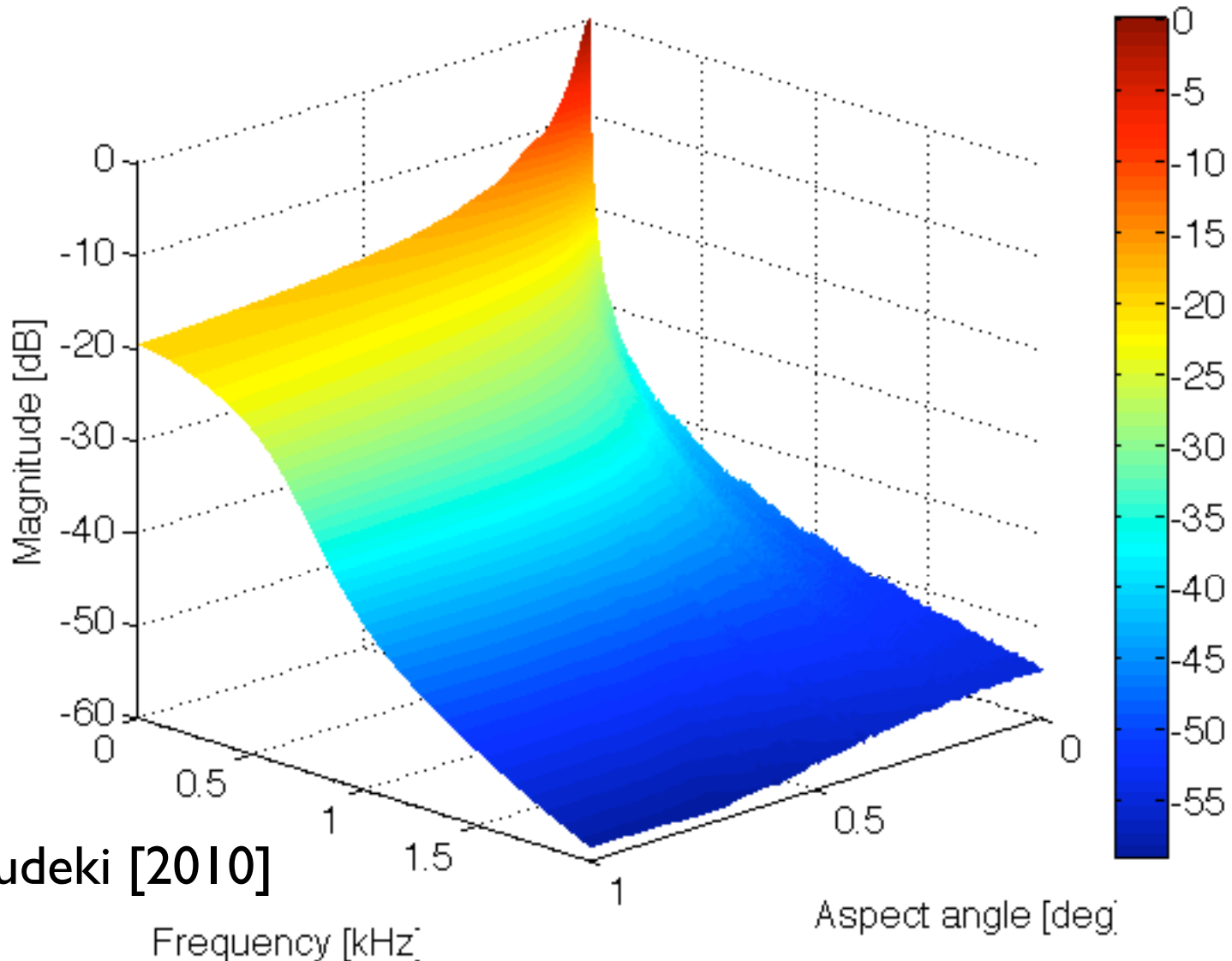


Electron temperature dependence of the simulated IS spectrum for $\lambda_B=3\text{ m}$ at aspect angles $\alpha=0^\circ$ (left panels), $\alpha=0.02^\circ$ (central panels), and $\alpha=0.1^\circ$ (right panels) (Milla & Kudeki, 2010).



Collisional IS Spectrum

ISR Spectrum - Sweeping aspect angle

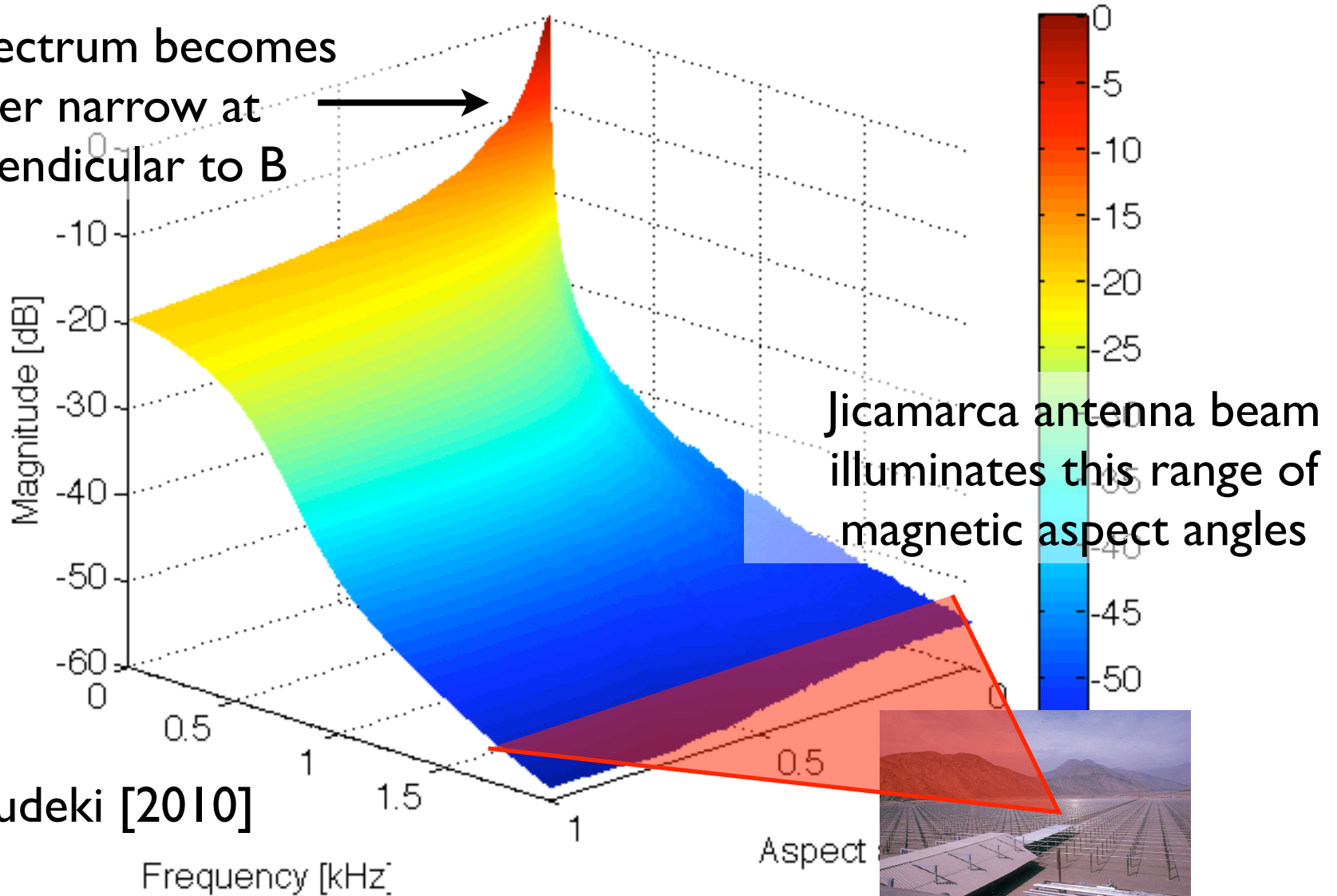




Collisional IS Spectrum

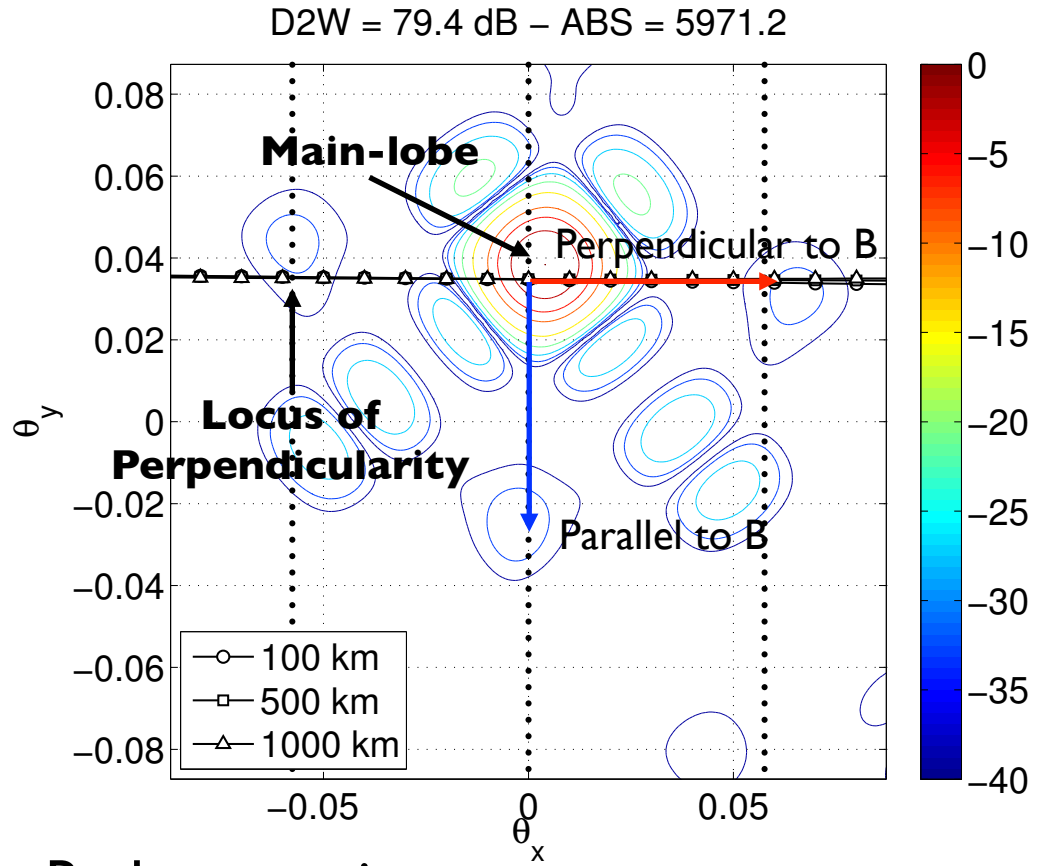
ISR Spectrum - Sweeping aspect angle

The spectrum becomes
super narrow at
perpendicular to B





Beam-weighted ISR spectrum

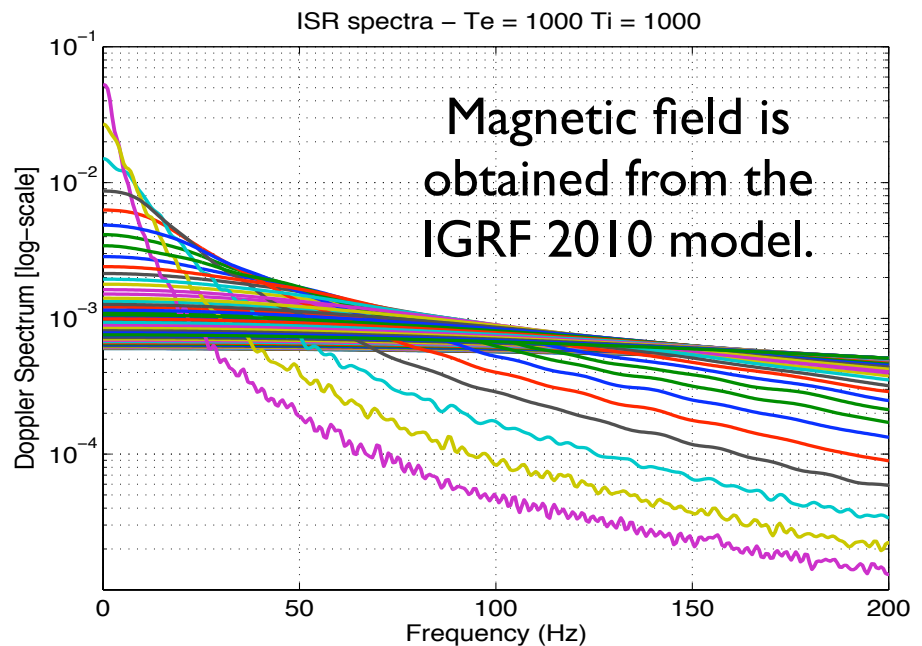


Radar equation:

$$\frac{S(\omega)}{E_t K} = \frac{\delta R}{R^2} \int d\Omega W(\hat{\mathbf{r}}) \sigma(\vec{k}, \omega)$$

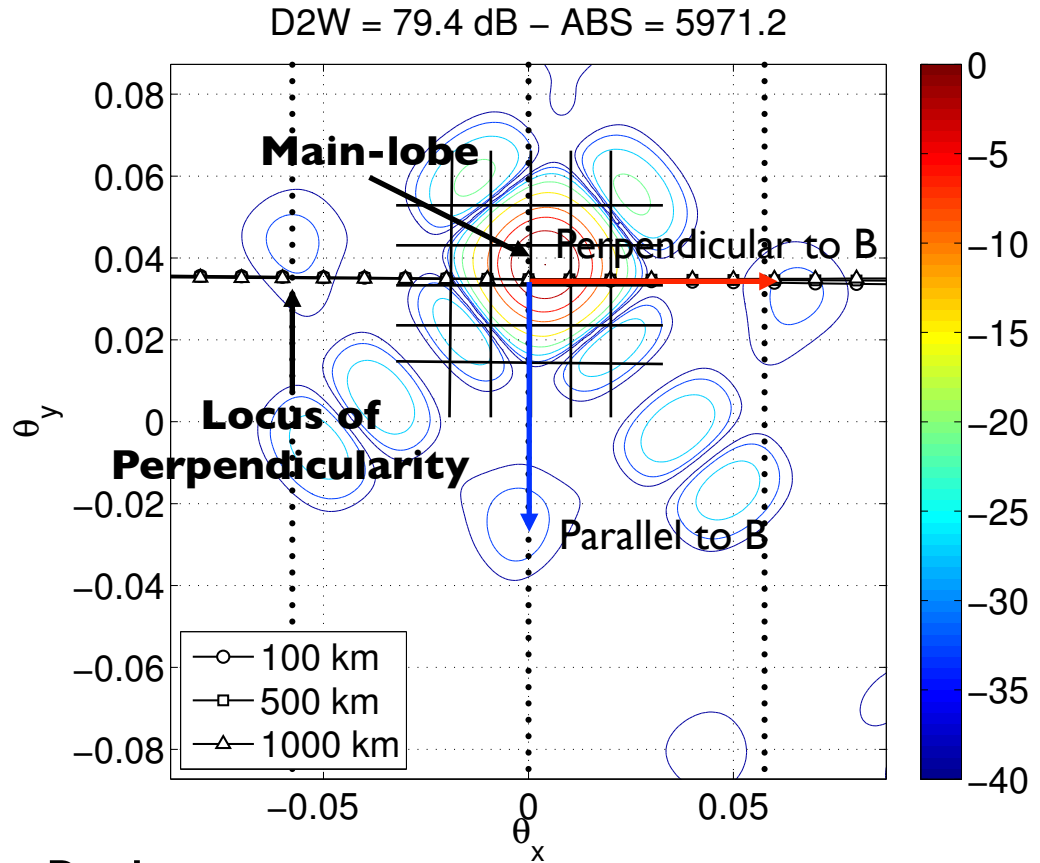
↑ IS-RCS $\rightarrow \sigma(\vec{k}, \omega) = 4\pi r_e^2 \langle |n_e(\vec{k}, \omega)|^2 \rangle$

- Jicamarca antenna beam pointed perp to B (beam-width: ~1 deg).
- The measured spectrum is the sum of the spectra corresponding to different magnetic aspect angles.





Beam-weighted ISR spectrum

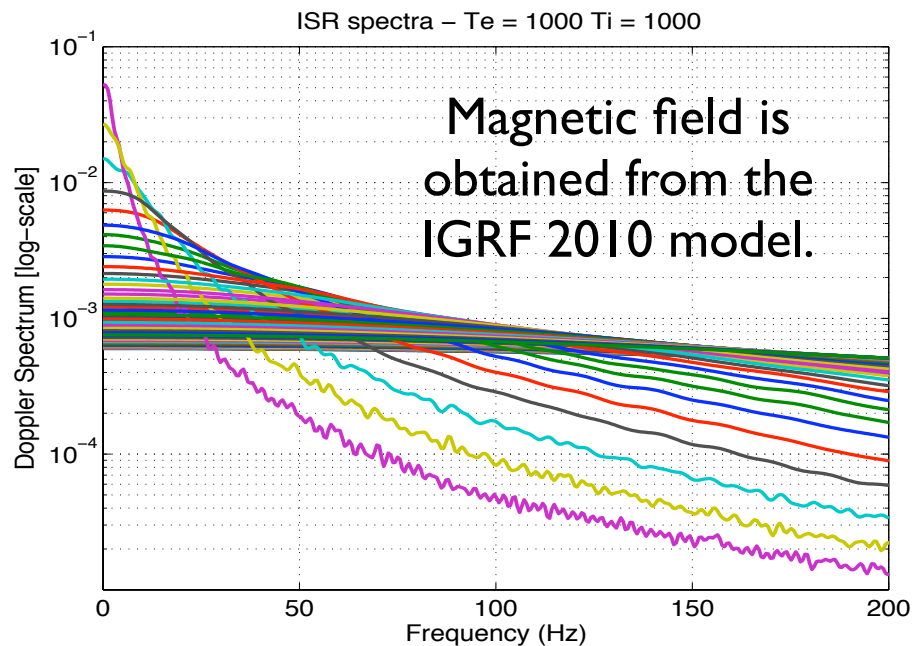


Radar equation:

$$\frac{S(\omega)}{E_t K} = \frac{\delta R}{R^2} \int d\Omega W(\hat{\mathbf{r}}) \sigma(\vec{k}, \omega)$$

↑ IS-RCS $\rightarrow \sigma(\vec{k}, \omega) = 4\pi r_e^2 \langle |n_e(\vec{k}, \omega)|^2 \rangle$

- Jicamarca antenna beam pointed perp to B (beam-width: ~1 deg).
- The measured spectrum is the sum of the spectra corresponding to different magnetic aspect angles.



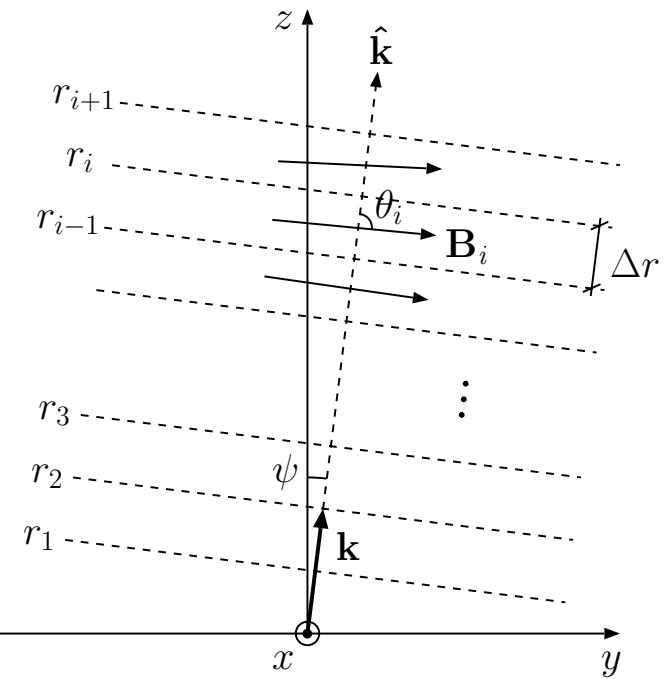


Second stage:

Modeling the magneto-ionic propagation
effects on the beam-weighted
incoherent scatter radar spectrum



Magneto-ionic propagation model (I)



Geometry of wave propagation in an inhomogeneous magnetized ionosphere.

Appleton-Hartree Solution

$$\begin{aligned}
 Y_L &= Y \cos \theta, & Y_T &= Y \sin \theta, & Y &= \frac{\Omega}{\omega}, & X &= \frac{\omega_p^2}{\omega^2} \\
 F_O &= F_1 - F_2, & F_X &= F_1 + F_2, & F_1 &= \frac{Y_T^2/2}{1-X}, & F_2^2 &= F_1^2 + Y_L^2 \\
 n_{O,X}^2 &= 1 - \frac{X}{1-F_{O,X}} \\
 \Delta n &= \frac{n_O - n_X}{2} & \bar{n} &= \frac{n_O + n_X}{2} & a &= \frac{F_O}{Y_L}
 \end{aligned}$$

$$\begin{bmatrix} E_\theta^i \\ E_\phi^i \end{bmatrix} = \underbrace{\frac{e^{-jk_o\bar{n}r}}{1+a^2} \begin{bmatrix} e^{-jk_o\Delta nr} + a^2 e^{jk_o\Delta nr} & 2a \sin(k_o\Delta nr) \\ -2a \sin(k_o\Delta nr) & a^2 e^{-jk_o\Delta nr} + e^{jk_o\Delta nr} \end{bmatrix}}_{\bar{T}_i} \begin{bmatrix} E_\theta^{i-1} \\ E_\phi^{i-1} \end{bmatrix}$$

Backscattered electric field for every propagation direction

$$\rightarrow \vec{E}_o^r \propto \kappa_i \underbrace{\bar{T}_1 \bar{T}_2 \cdots \bar{T}_i \bar{T}_i \cdots \bar{T}_2 \bar{T}_1}_{\bar{\Pi}_i} \vec{E}_o^t$$

Two-way propagator matrix



Magneto-ionic propagation model (2)

Soft-Target Radar equation:

$$\frac{S(\omega)}{E_t K} = \frac{\delta R}{R^2} \int d\Omega W(\vec{r}) \sigma(\vec{k}, \omega) \quad \sigma(\vec{k}, \omega) = 4\pi r_e^2 \langle |n_e(\vec{k}, \omega)|^2 \rangle$$

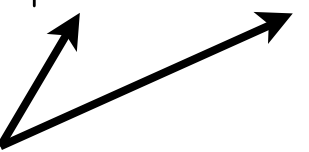
But now, $W(\vec{r})$ is an effective two-way radiation pattern

$$W(\vec{r}) = \frac{1}{k^2} G_t(\hat{\mathbf{r}}) G_r(\hat{\mathbf{r}}) \Gamma(\vec{r})$$

where $\Gamma(\vec{r})$ is a polarization coefficient

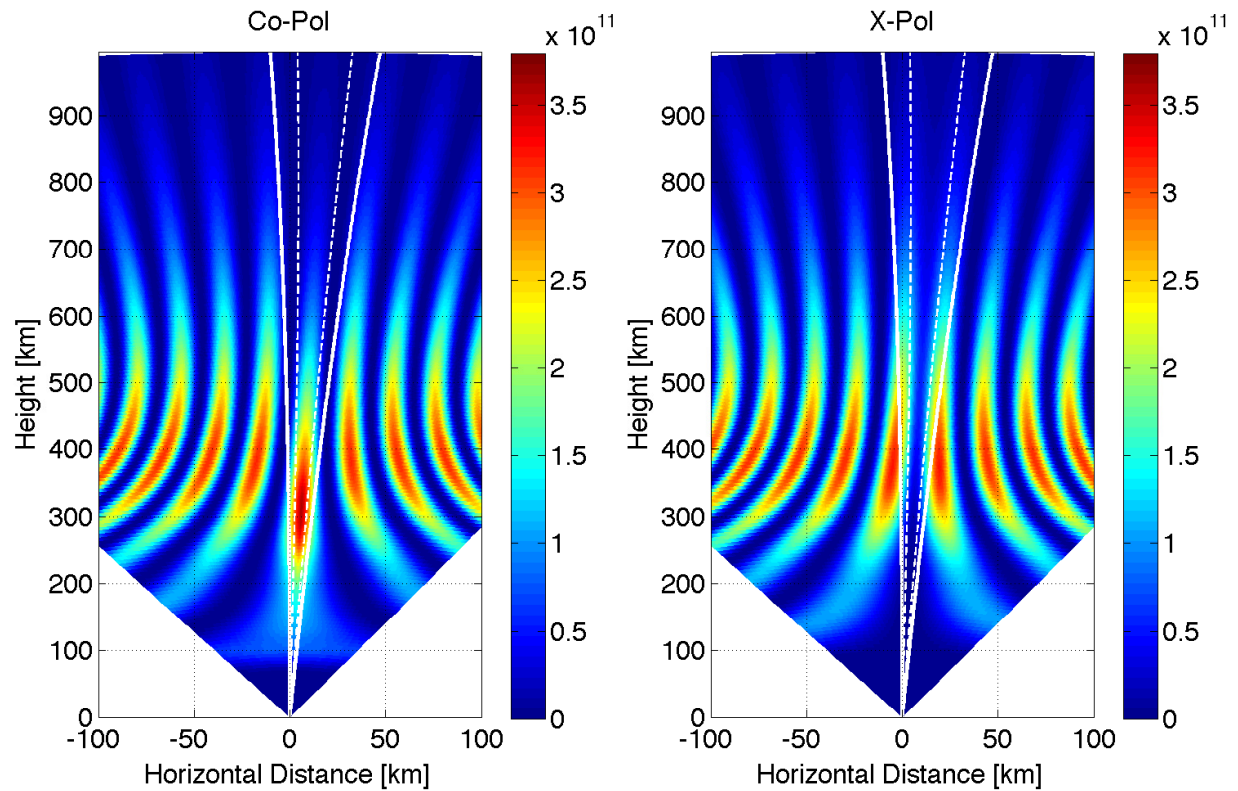
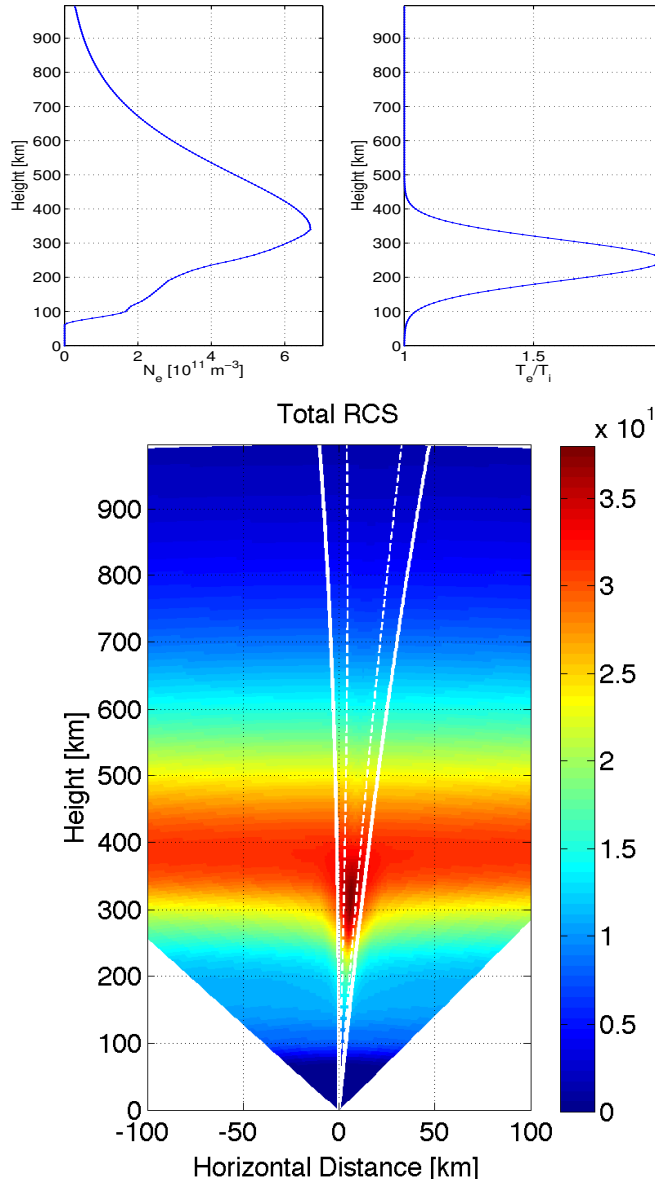
$$\Gamma(\vec{r}) = |\hat{\mathbf{p}}_r^\top \bar{\Pi}(\vec{r}) \hat{\mathbf{p}}_t|^2$$

polarization unit vectors





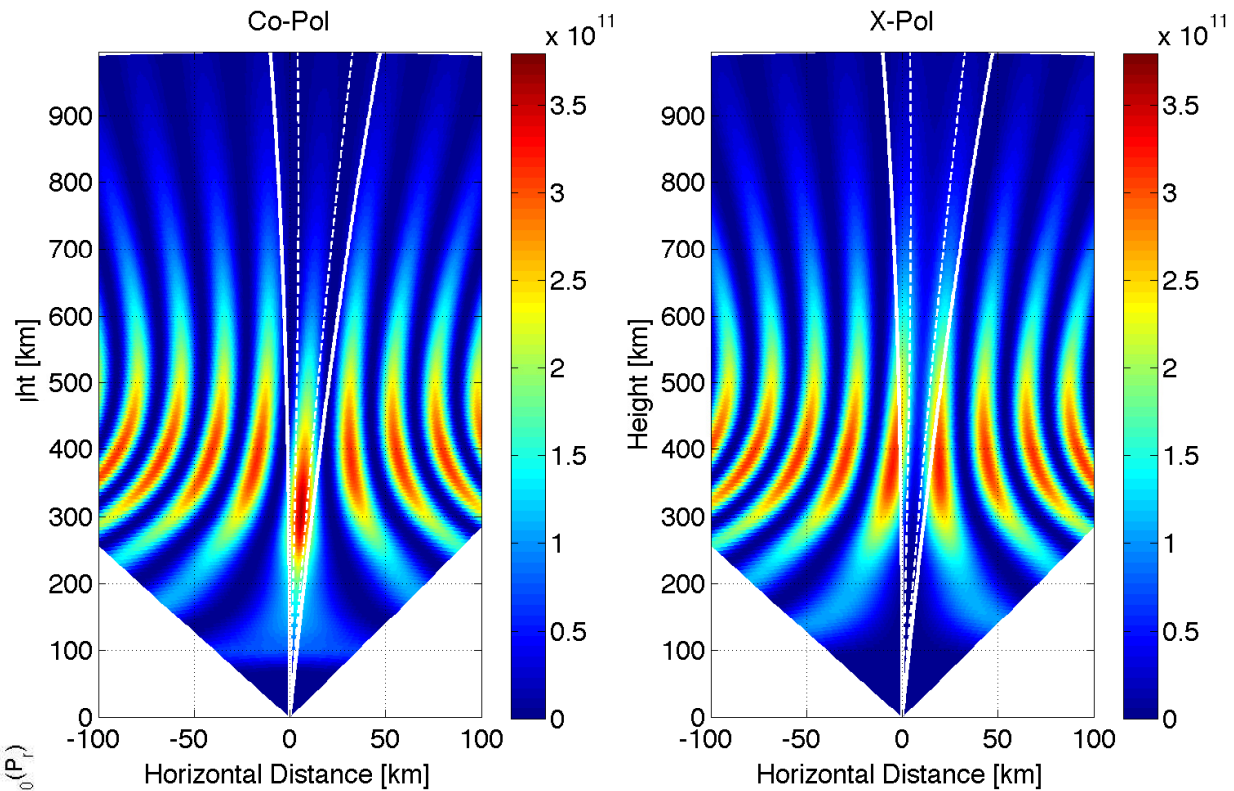
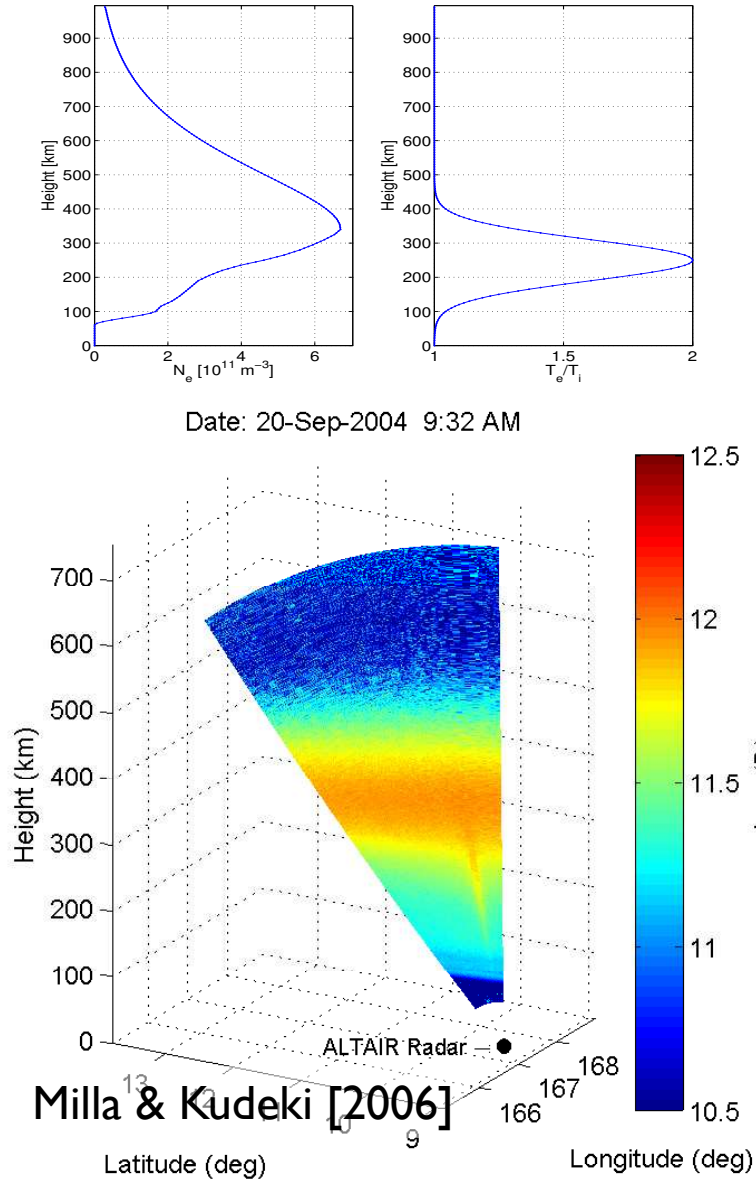
Magneto-ionic propagation model (3)



Co-polarized, cross-polarized, and total backscattered power detected by a pair of orthogonal linearly polarized antennas.



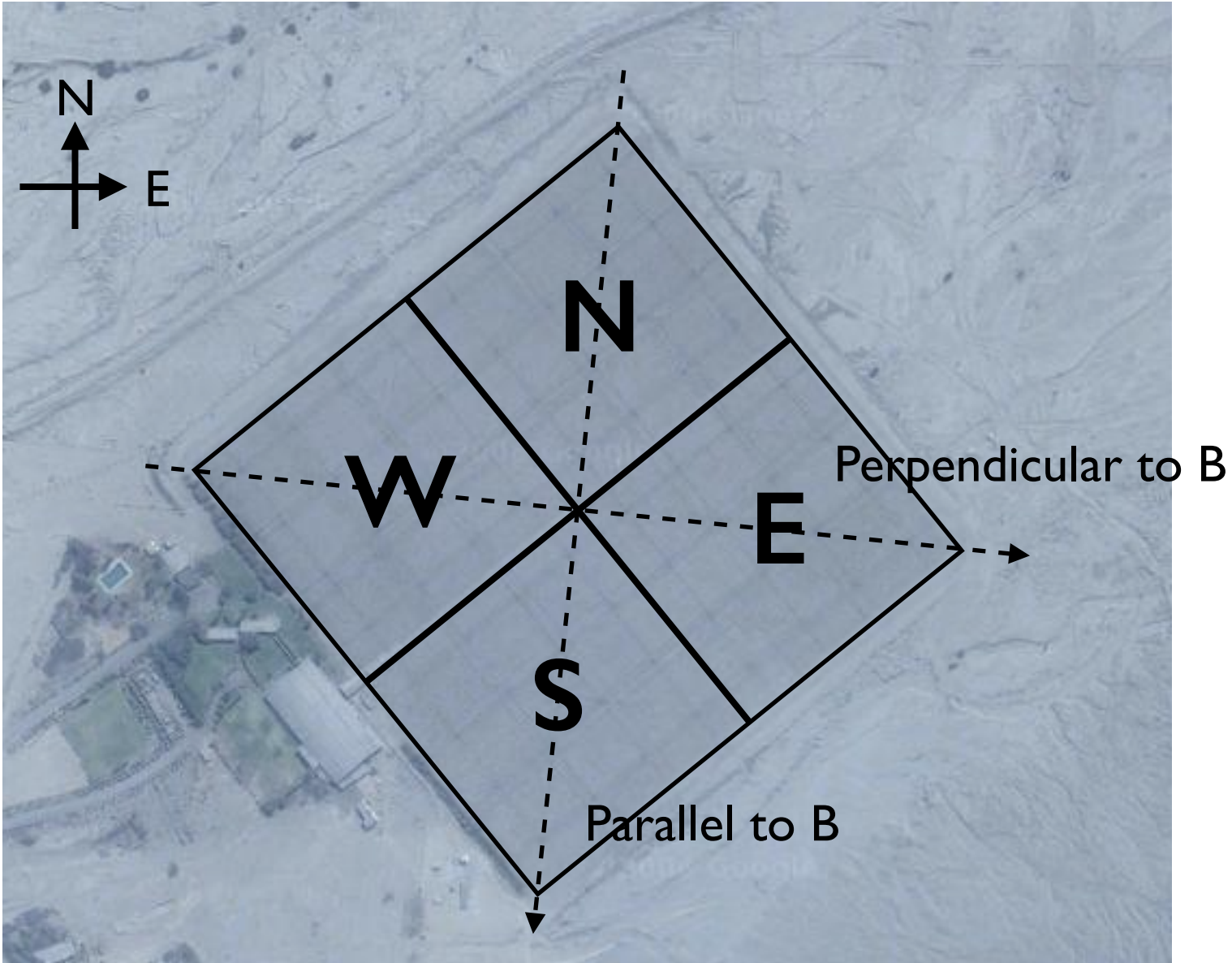
Magneto-ionic propagation model (3)



Co-polarized, cross-polarized, and total backscattered power detected by a pair of orthogonal linearly polarized antennas.

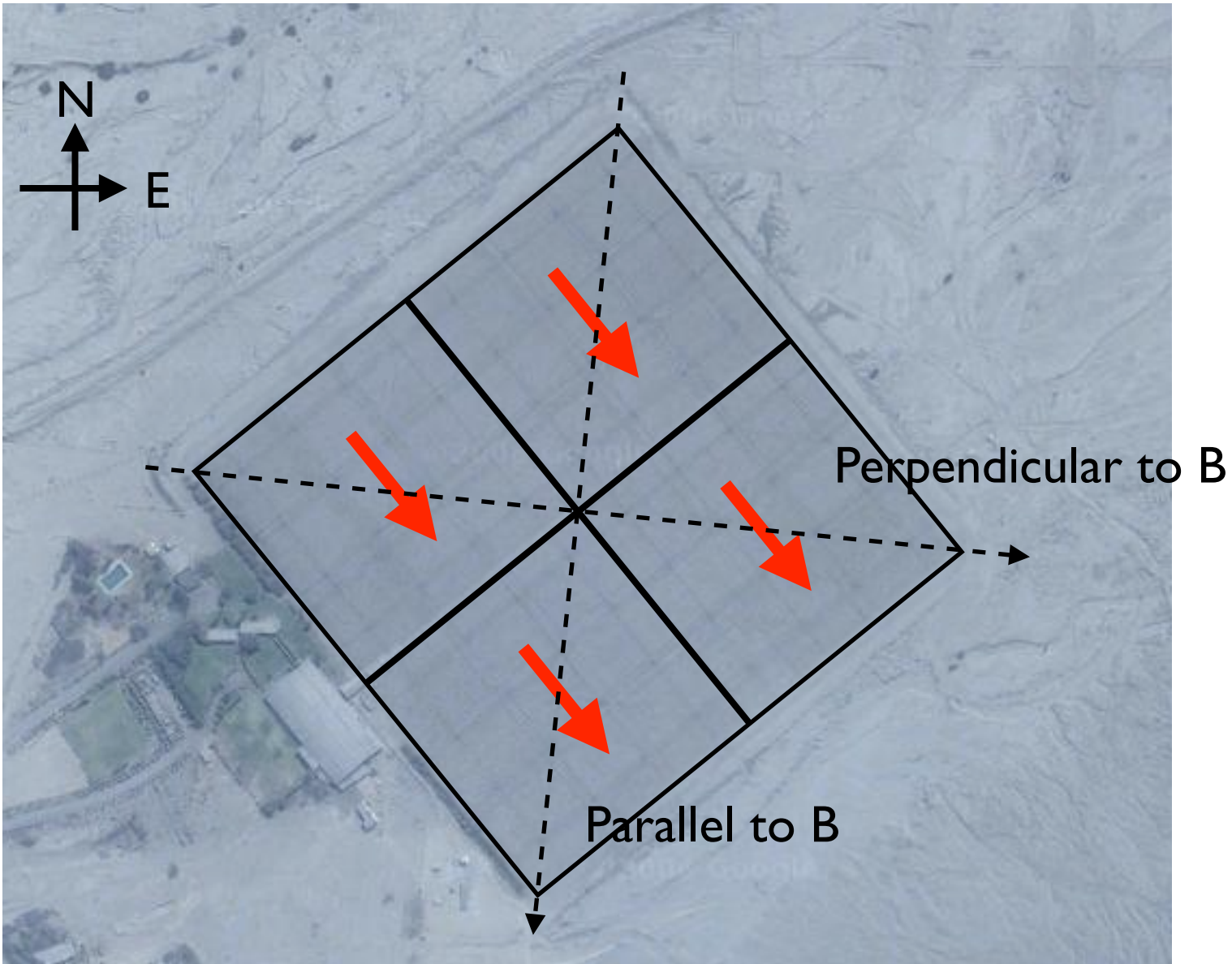


Application: Differential-phase experiment



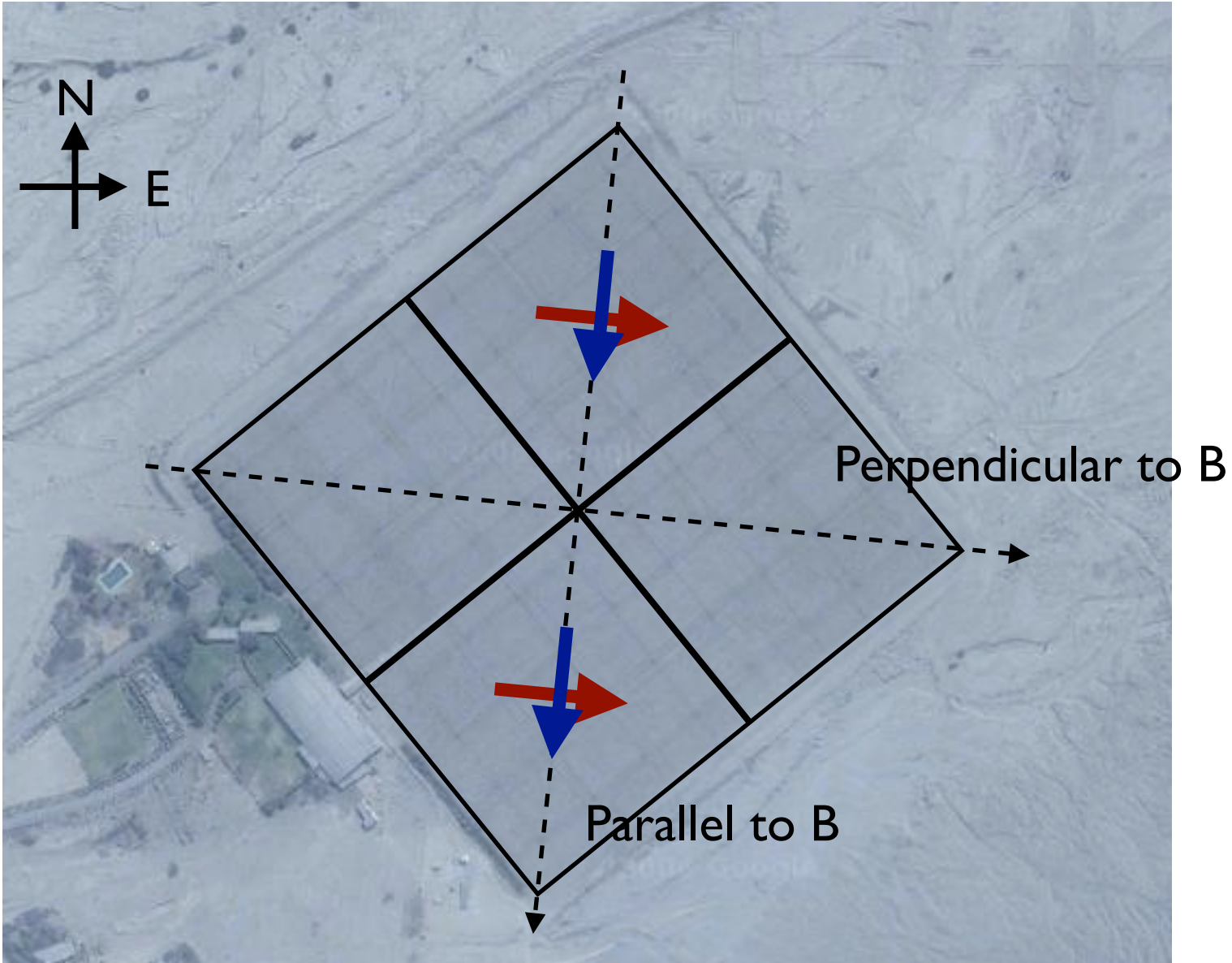


Application: Differential-phase experiment



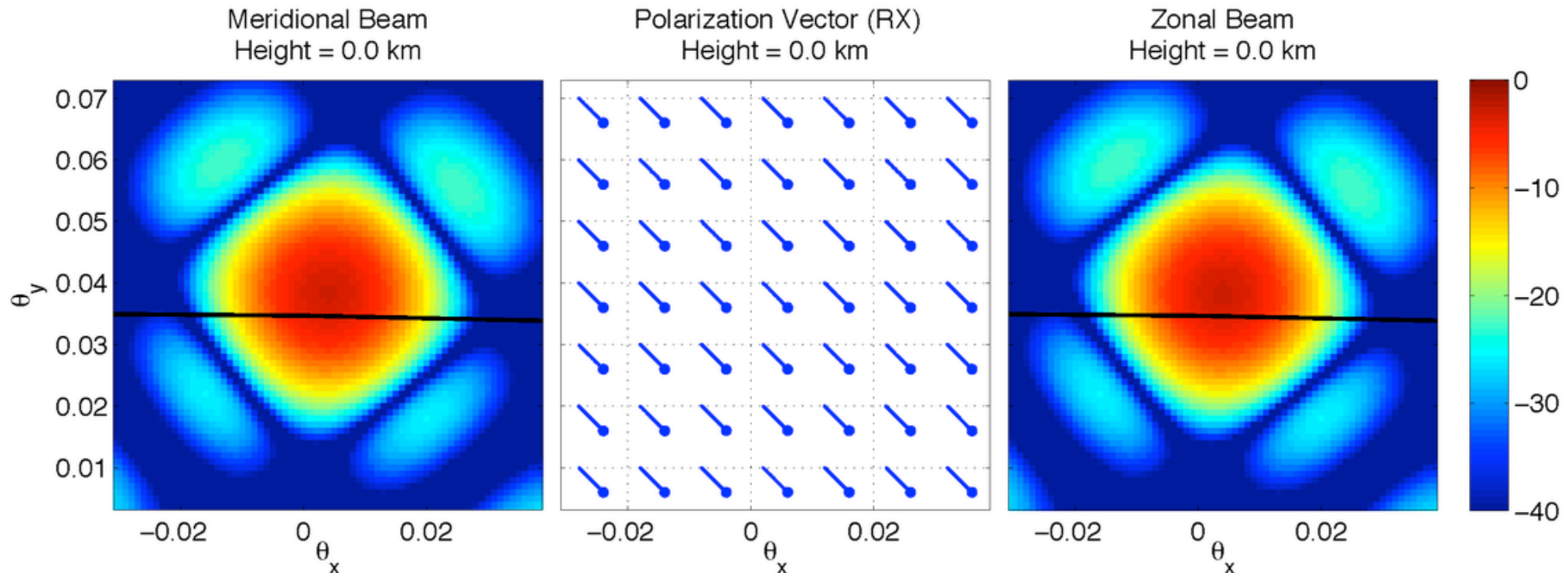


Application: Differential-phase experiment





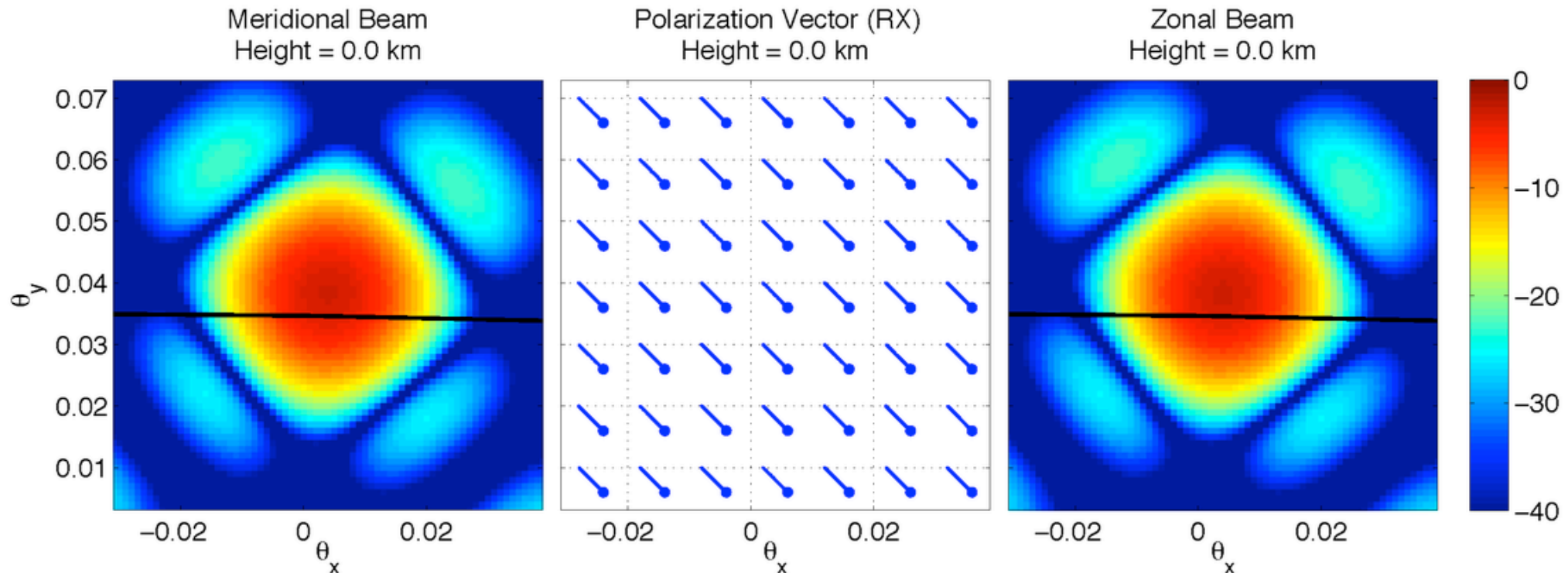
Beam-shape modified by magneto-ionic propagation effects



Simulation



Beam-shape modified by magneto-ionic propagation effects



Simulation

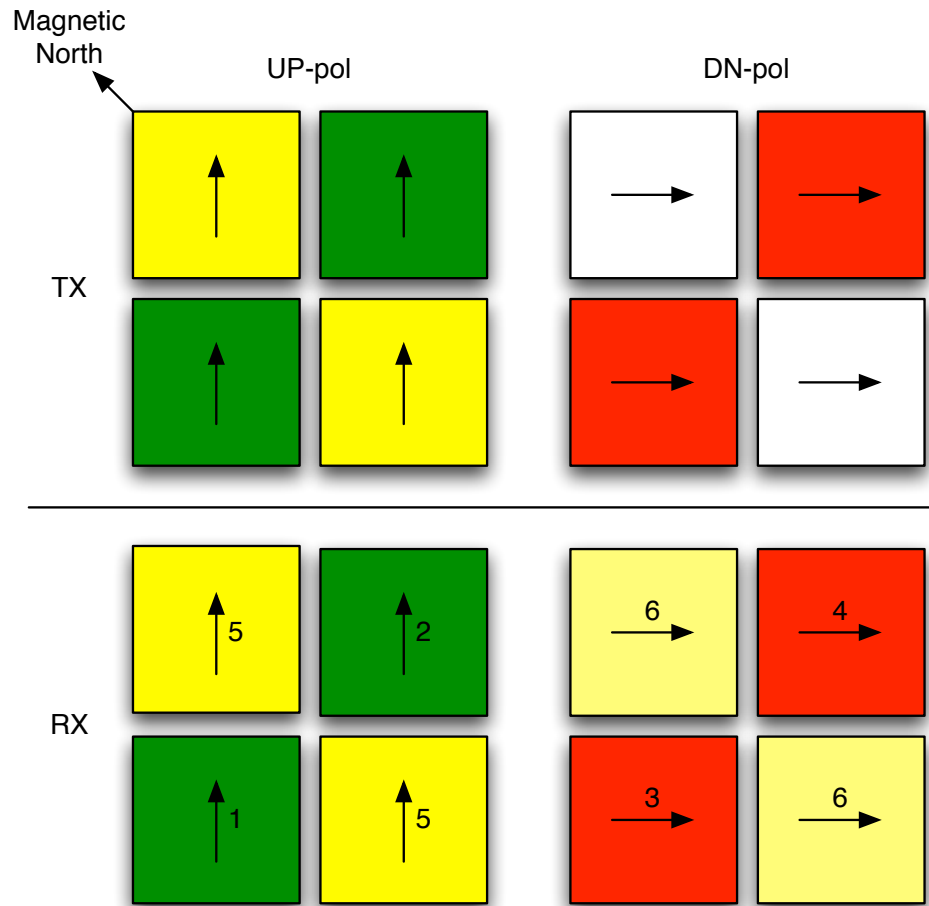


Application:

3-Beam radar experiment and
estimation of N_e and T_e/T_i profiles

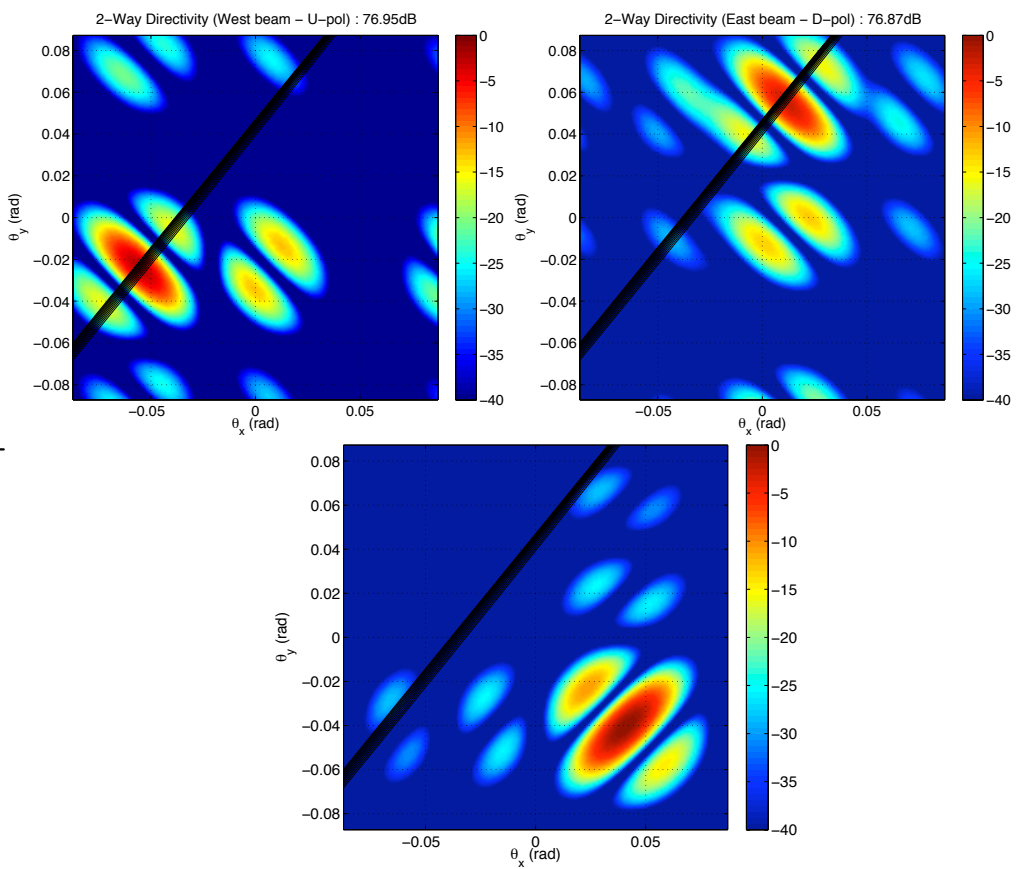


3Ba antenna configuration



RX1 WU: West 1 (Quarter)
RX2 EU: West 2 (Quarter)
RX5 SU-NU: South (Co-Pol)

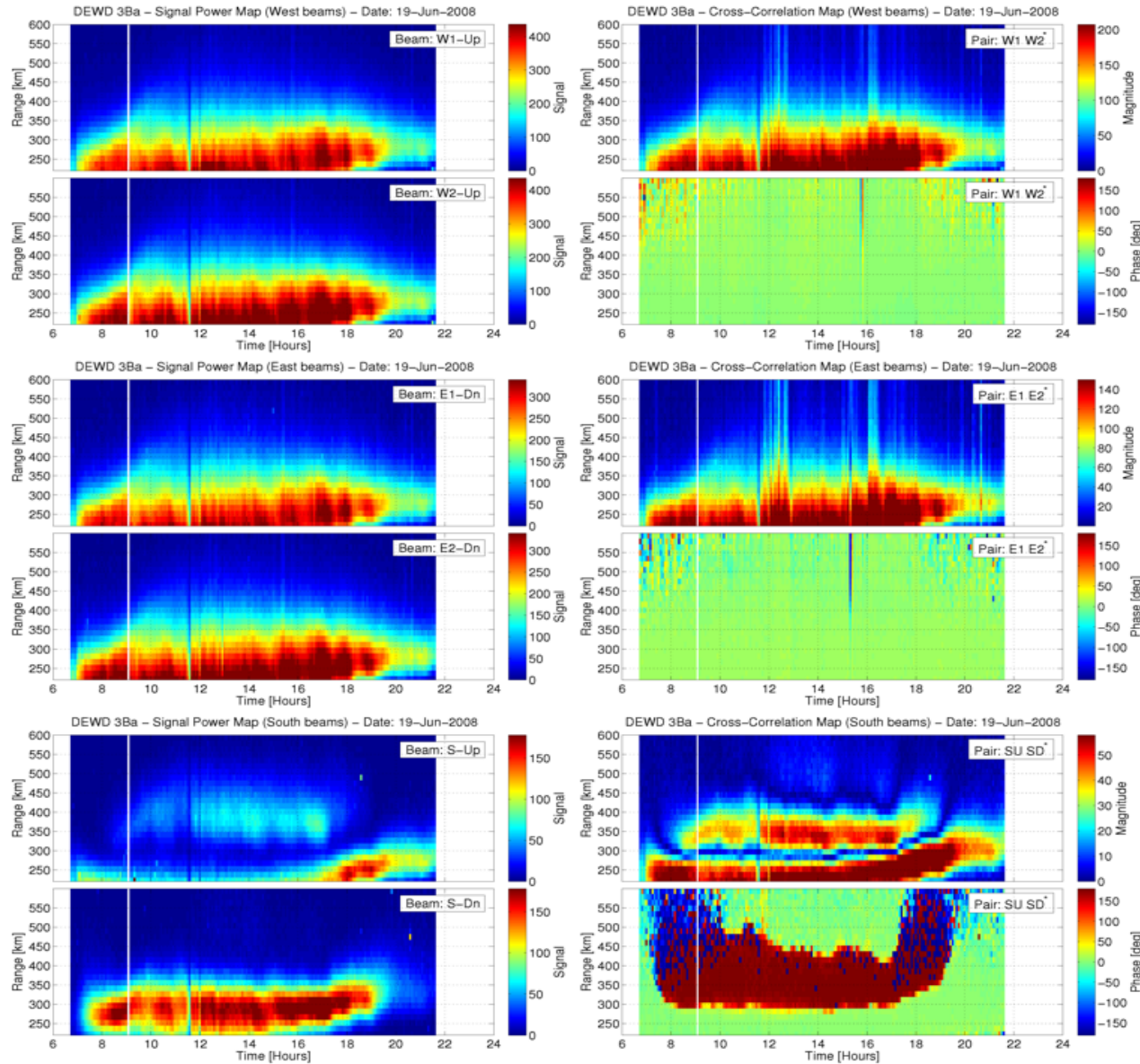
RX3 WD: East 1 (Quarter)
RX4 ED: East 2 (Quarter)
RX6 SD-ND: South (X-Pol)



West, east, and south
radiation patterns



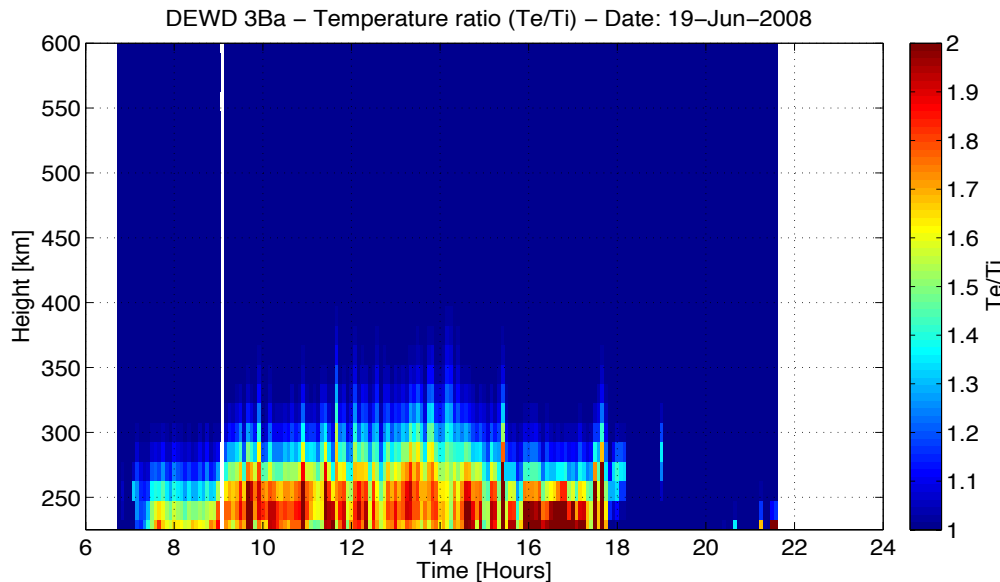
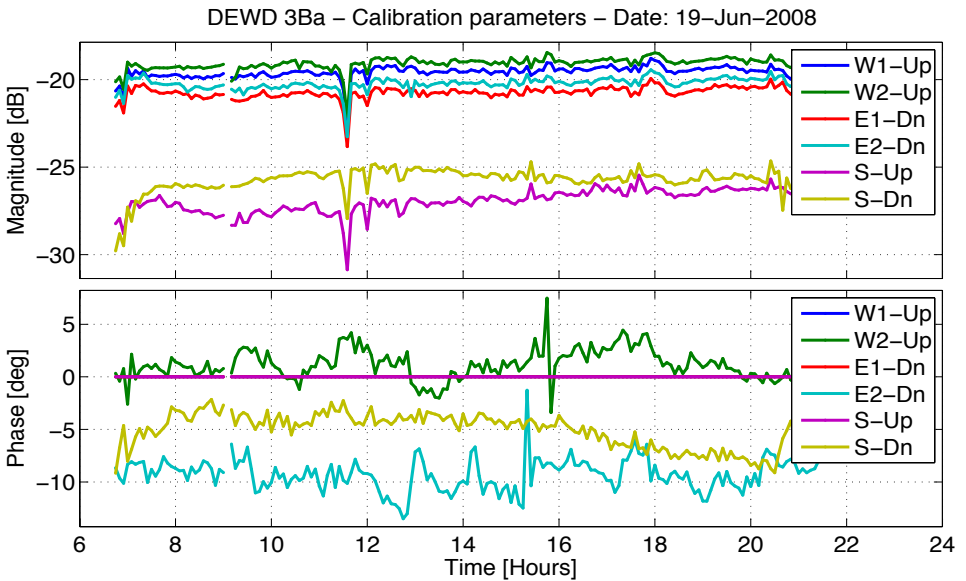
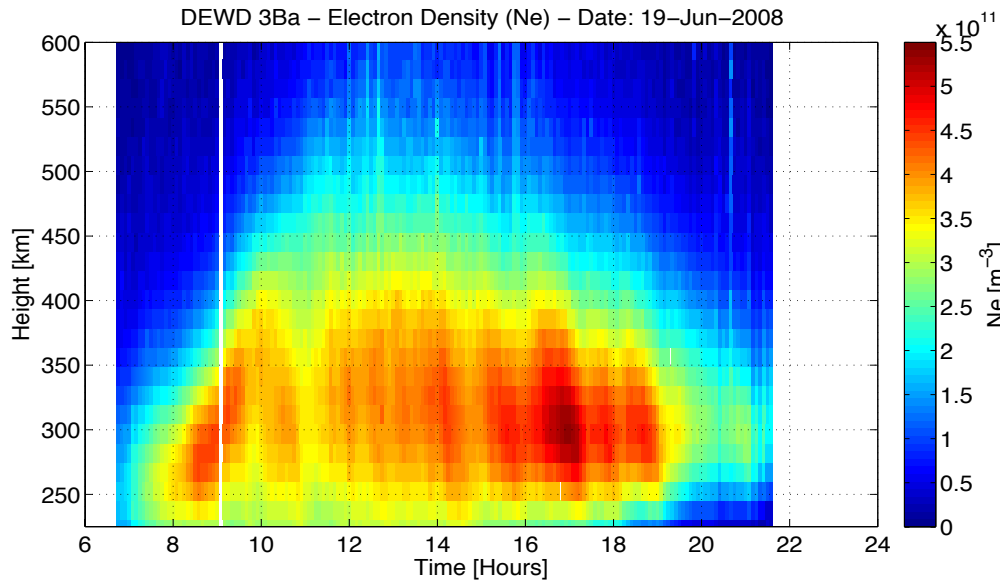
Power and cross-correlation measurements



- Range vs. time plots of the signal power and cross-correlation data measured in the 3Ba experiment of June 19, 2008.
- On the left, the power data collected by each of the radar beams are displayed in linear scale.
- On the right, the magnitudes of the cross-correlation data are also plotted in linear scale, while the phase data are plotted in degrees.



Inversion results



Estimated parameters

- Electron densities
- T_e/T_i profiles
- Calibration parameters



Conclusions and Future work

- The modeling of the perpendicular-to-B IS spectrum measured by the Jicamarca radar needs to consider:
 - Electron and ion Coulomb collisions effects
 - Magneto-ionic propagation effects
 - Beam-weighting effects
- We have developed the tools to model these effects, but still need to optimize our procedure for routine operational use.
- We also need to study in more detail the sensitivity of our model to plasma temperatures and densities.
- Our model was developed for an O⁺ plasma, we need to extend our model to H⁺ and He⁺ plasmas for radar observations of the topside.
- Spectral fitting for Te estimation should now be possible given the Te/Ti profiles and the development of our collisional ISR spectral model.